UNIVERSITY OF CALIFORNIA

Santa Barbara

Linear Low Density Polyethylene Polymerization over Single Site Organometallic Catalysts and Mechanistic Insights into the Comonomer Effect

A dissertation submitted in partial satisfaction of the requirements for the degree Doctor of Philosophy in Chemistry

by

Joshua Maxwell Speer

Committee in charge:

Professor Mahdi M. Abu-Omar, Chair

Professor Armen Zakarian

Professor Trevor W. Hayton

Professor Gabriel Ménard

December 2023 The dissertation of Joshua Maxwell Speer is approved.

_____

Armen Zakarian

_____

Trevor W. Hayton

_____

Gabriel Ménard

Mahdi M. Abu-Omar, Committee Chair

December 2023

Linear Low Density Polyethylene Polymerization over Single Site Organometallic Catalysts and Mechanistic Insights into the Comonomer Effect

ACKNOWLEDGMENTS

I would like to start by acknowledging my parents, Dr. Drew and Nanci Speer, without their never ending patience for my never ending string of "… But why?" I would not have grown into the type of curious man that endlessly pursues answers.

I would also like to thank the chemistry professors at Ithaca College. Receiving an undergraduate education at a school with such a low student to faculty ratio meant that every professor I knew had an impact on me and helped me grow into the scientist that I am today. A special thanks goes to Dr. Janet Hunting who was the first professor to oversee my independent research. I studied in her lab for almost 3 years learning how exciting, and frustrating, research truly was. She motivated me to ask my own questions and search for my own solutions. Additionally, I would like to thank Dr. Anna Larsen who patiently worked with me to improve my writing skills for my senior thesis at IC.

My education at the University of California, Santa Barbara has been an amazing opportunity to provide me with quality guidance and the tools to keep asking, and answering, interesting questions. I'd like to thank Dr. Mahdi Abu-Omar for being my research advisor through the good times and the bad; I never thought I would spend this much time in graduate school but then Covid-19 came along and put the world on pause. Mahdi has always seen the best in me and pushed me to achieve that, he has made me into the scientist I am today. I would like to extend thanks to the rest of my committee members also, Dr. Armen Zakarian, Dr. Trevor Hayton, and Dr. Gabriel Ménard for serving on my committee during my time at UCSB.

I am also extending thanks to my collaborators at Purdue University, Dr. Jim Caruthers, Dr. Grigori Medvedev, and Dr. Jeffrey Switzer whose perspective from a chemical engineer helped expand both my capacity to understand and explain complex topics in simple terms. Without their help building the kinetic model in Chapter III would not have been possible and our long discussions of the error within our error bars helped keep me sane while locked down for the pandemic.

I would like to thank all members of the Abu-Omar group, past and present, for being my friends and colleagues. I am grateful for Dr. Chan Park for first taking me under his wing when I initially joined the lab, as well as Dr. Baoyuan Liu for training me on the PARR and GC-FID systems. Although not a part of the Abu-Omar group I have worked closely with Dr. Nick Maciulis and thoroughly enjoyed his company as well as bouncing ideas off of.

Finally I'd to thank my partner, Olivia Bourke, for her love and support. I would not have made it this far without her to lean on, thank you for believing in me even when I was unable to believe in myself.

Table of Contents

CHAPTER I. Ethylene Polymerization

A. Ziegler Natta Catalysts

Polyethylene is an important consumer product. Of the 400 million metric tons of total plastics produced annually, 100 million metric tons is polyethylene, making it the largest plastic in use[1]. Part of the reason polyethylene is used in so many consumer products has to do with its versatility. High density polyethylene (HDPE) is a stiff but pliable solid that can be easily pressed into shape at high temperature hold its mold at room temperature. In HDPE the polymer chains pack very efficiently having semi-crystalline domains of polyethylene in its thermodynamically favored staggered confirmation with amorphous regions of entangled polymer that yield a firm but flexible plastic (Figure 1.1). In contrast low density polyethylene (LDPE) contains very few crystalline regions and is instead a clear, flexible, soft plastic. In practice this is achieved by introducing either short or long chain branches to the polymer. Long chain branching was the first method discovered and utilizes a free radical process at high pressure to randomly distribute another growing chain onto the polymer chain[2]. Of more interest to academic research are short chain branches, because these branch points are smaller in chain length there need to be more of them before interesting effects on polymer properties such as lower T_m are seen. In practice this means a ^{13}C NMR can be fully assigned, due to both the abundance and regularity of chain branches. All catalysts that are active for ethylene polymerization will also polymerize alpha-olefins;

the most industrially relevant comonomers are 1-butene, 1-hexene, and 1-octene due to the availability of these monomers. Because reaction systems such as these give a LDPE that is a linear chain with well defined short chain branches it is often referred to as linear low-density polyethylene (LLDPE). The properties of LLDPE depend primarily on the concentration of branch points and can be controlled easily on an industrial scale by varying the content of the alpha-olefin in the feed[3].

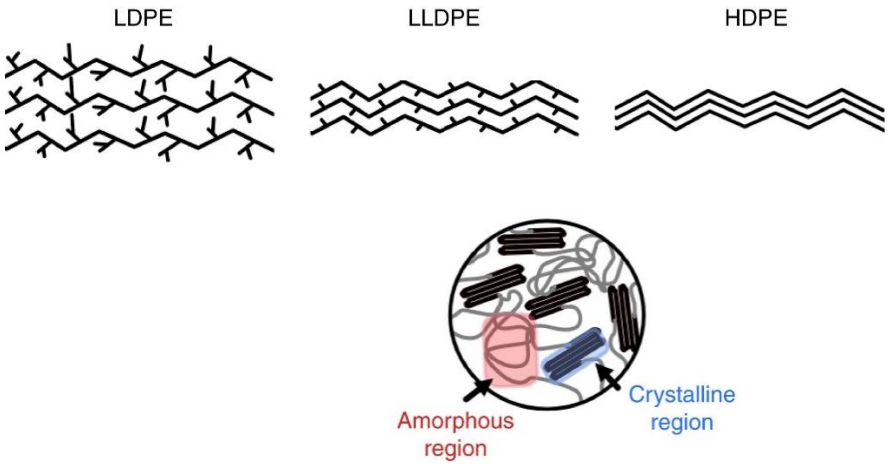

Figure 1.1 Staggered microstructures of the semicrystalline regions of LDPE (left), LLDPE (middle) and HDPE (right) with schematic depicting amorphous regions and crystalline regions in the macrostructure[4].

One half share of the 1963 Nobel Prize in Chemistry was awarded to Karl Ziegler for his work in developing organometallic catalysts that enabled new polymerization reactions, primarily the reaction of ethylene to polyethylene. These catalysts were titanium halides that when reacted with organoaluminium species, such as triethylaluminium, would produce alkylated titanium which would polymerize ethylene at relatively mild temperature and pressure. Catalysts supported by $MgCl_2$ would eventually be developed to be so active that purifying the used catalyst from the polymer wasn't necessary and therefore lead to the

industrial adoption of polyethylene as a cheap to manufacture plastic, a practice that continues today[5-6].

B. Metallocene Catalysts

Mechanistic studies into the original Ziegler-Natta catalysts were difficult because of issues identifying what the catalytically active species is, and in many cases no single site was found but rather many active sites/species. The first Ziegler-Natta catalyst derivative to have the mechanism widely agreed upon (Scheme 1.1) was for titanocene dichloride, Cp_2TiCl_2, and utilized methylaluminumoxane, MAO, as an activator[7]. It was found that the active species was cationic Cp_2TiMe^+, having lost both chlorides and gained a methyl from MAO. This species is a good enough electrophile to coordinate ethylene and insert a methyl into it, generating $Cp_2Ti(CH_2CH_2CH_3)^+$ which can continue to propagate ethylene insertions, growing a linear chain by two carbon atoms each time.

Scheme 1.1 Mechanism of ethylene polymerization by Cp_2TiCl_2 and MAO cocatalyst to afford HDPE[8]

C. Single Site Homogenous Catalysts

In the late 1990's polyolefin catalysts expanded from metal alkyl or metallocene based catalysts towards coordination complexes with oxygen and nitrogen as donor ligands. Amine donors were found to be more susceptible to varying polymerization conditions. For

example, the solvent was found to have a large impact on activity for early catalysts, likely because of interactions with the cationic active metal site(s). These limitations were overcome by using alkanes as solvent or using bulkier activators like MMAO (modified methylaluminumoxane) or $B(C_6F_5)_3$. One design motif that leads to very active catalysts is the mixing of amine and imine bonds in Zr or Hf complexes.[9]

Kinetic analysis of single site catalysts was made possible by the use of boron compounds, primarily $B(C_6F_5)_3$ (BCF), acting as Lewis acids (Scheme 1.2). Since boron is less reactive than aluminum it is not sufficient to remove chlorides and replace them with alkyl groups, however, it can abstract an alkyl group. The main advantage is that since these types of boron compounds are molecular species they generate only one active catalyst instead of multiple active sites. This allows rate constants to be specified for individual catalysts and other structure-activity relationships to be studied. In one example[10] researchers found that while the rate of initiation (k_i) and propagation (k_p) varied by catalyst, the ratio k_i/k_p only varied on ligand cone angle, where a more sterically restricted active site had a lower k_i/k_p, it was more difficult to initiate.

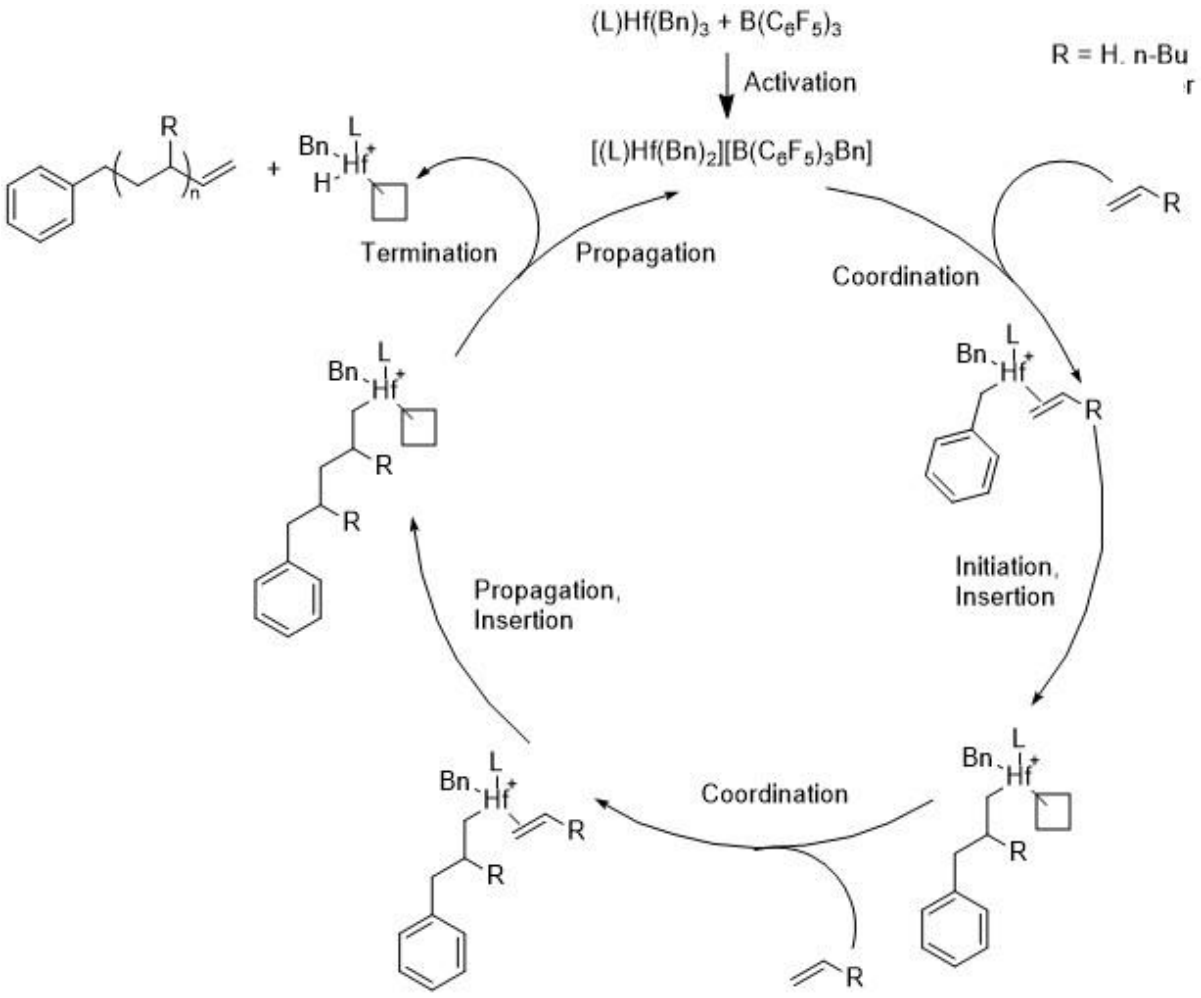

Scheme 1.2 Activation and initiation of a generic single site hafnium catalyst by BCF and subsequent polymerization.

Studies of these catalyst systems have also eluded information on how the electronics of a support ligand effects the mechanism of polymerization. A family zirconium amine bis-phenolate catalysts that only differed by a pendant ligand, a ligand which could coordinate a lone pair with the zirconium or dangle freely leaving the zirconium under-coordinated, was studied for 1-hexene polymerization.[11] The pendant ligand to zirconium bond distance was measured by crystallization of the precatalyst followed by X-Ray Diffraction (XRD), and kinetic rate constants were obtained by measuring monomer consumption, molecular weight

distribution evolution and direct observation of the chain termination products by ^{1}H NMR. The study found that complexes with shorter pendant ligand to zirconium bond were less likely to undergo chain termination events and therefore produced higher molecular weight polymer[11]. In addition, softer ligands like sulfur and furan primarily underwent β-H transfer for the termination of a growing polymer chain while harder ligands like nitrogen and tetrahydrofuran primarily underwent β-H elimination as the terminal event.

D. The Comonomer Effect

Across many different polymerization catalysts and in many different reaction systems it is observed that the introduction of a small amount of α-olefin dramatically increases the amount of polymer produced, far more than can be explained by the added mass of α-olefin.[12] This tendency for catalysts to show enhanced reactivity towards ethylene in the presence of an α-olefin has been coined the 'comonomer effect'. So far, no mechanism for the comonomer effect has been able to explain the increase in productivity broadly in all systems. The explanations for the comonomer effect are either physical, relating to differences in productivity to physical properties of the resulting polymer, or chemical where the α-olefin modifies the catalyst or affects the rate constants directly.

In the case of heterogenous catalysis, the growth of the polymer particle has been extensively studied[13,14] for its connection to the comonomer effect. Heterogenous catalysis in general can have issues with self-fouling where the growing polymer chain collapses upon the catalyst/support structure and effectively forms an impenetrable barrier between solution state ethylene and active sites. This can be studied by a technique pioneered for the polyolefin characterization field: Crystallization Analysis Fractionation (CRYSTF) which is

analogous to Differential Scanning Calorimetry (DSC) except crystallization is directly measured by an IR detector instead of inferred from heat flow. CRYSTF analysis shows that the introduction of 1-hexene to the reaction system causes the onset of crystallization to be depressed by up to 35 °C. The polymers were also analyzed under scanning electron microscopy (SEM), polymers formed in the absence of 1-hexene had fully enveloped the solid-state support while copolymers showed signs of fragmentation of the polymer shell (Figure 1.2). Fragmentation is crucial to maintaining productivity in longer reactions because it allows monomers to access the active site. Polyethylene forms semi-crystalline domains where the majority of polymer can adopt its thermodynamically favored staggered position however, the incorporation of 1-hexene adds a tertiary carbon and short butyl chain that effectively acts as a crystal defect, preventing large impermeable crystalline domains from forming and blocking active sites from monomer.

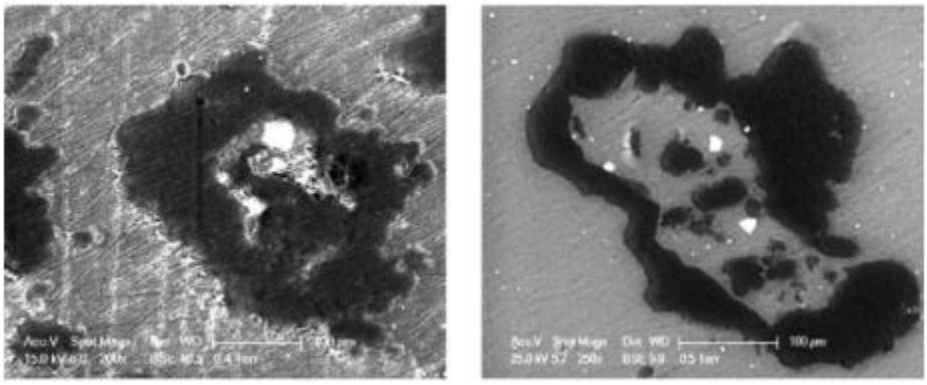

Figure 1.2 SEM images of polyethylene (left) fully surrounding an active site and copolymer (right) with fragmentation of the polymer particle.[14] Darker areas are polymer and lighter areas are catalyst.

It has also been reported that the introduction of an α-olefin modifies the active site, generating a new, more active, catalyst in situ. This has been studied[15] in the case of

homogenous catalysis where a metal-aryl bond exists, upon activation with $B(C_6F_5)_3$ either ethylene or 1-octene would insert into this bond, forming a metal-alkyl bond in its place before insertion into an alkyl group would initiate polymerization (Figure 1.3). The precatalyst was activated under the homopolymerization of either ethylene or 1-octene and then once a single active species was formed the other monomer was introduced to form copolymer. Results showed that when homopolymerization of ethylene was followed by copolymerization of ethylene and 1-octene a similar amount of polymer was formed as the copolymerization alone, however when homopolymerization of 1-octene was performed prior to copolymerization the overall rate of polymerization was a factor of three higher.

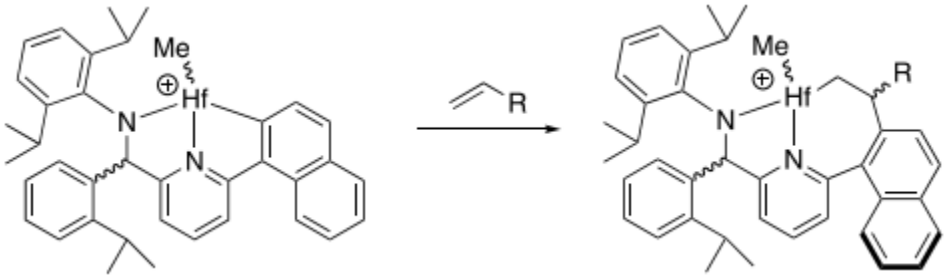

Figure 1.3 Insertion of ethylene (R = H) or 1-octene (R = C_6H_{13}) into an active catalyst prior to initiation[15].

Other such modifications of active sites have been suggested for heterogenous catalysis as well. In one example[16] five active sites were identified over a heterogenous $TiCl_4/SiO_2$ catalyst by applying a Flory–Schulz distribution to the polymer molecular weight distributions. The rate of catalysis in homopolymerization of ethylene and copolymerization of ethylene and 1-hexene over these five sites are shown in Table 1. The presence of 1-hexene increased the effective rate of reaction compared to ethylene alone, especially for the active centers that produce lower M_w polymer (Table 1.1).

Table 1.1 Rate of polymerization of ethylene and ethylene-hexene mixtures over a solid state supported Ti catalyst. Active centers are numbered in order of increasing M_w, such that Center I produces the lowest molecular weight polymer and Center V produces the highest molecular weight polymer.[16]

Active Centers	Rate (1/(g catalyst*min))		Percent Increase
	Ethylene Only	Ethylene + 1-Hexene	
I	0.034	0.205	+500 %
II	0.082	0.237	+190 %
III	0.128	0.443	+250 %
IV	0.211	0.247	+17 %
V	0.156	0.128	-18 %

Other chemical effects suggest that the α-olefin acts as a ligand, and the added steric bulk moves the cationic active site further from the boron anion which increases propagation rate. This effect was demonstrated in a study[17] of the copolymerization of propylene and 1-nonene and found that at lower temperatures the comonomer fraction in the copolymer increases, suggesting that the comonomer has a higher thermodynamic affinity to the active site despite the slower reaction kinetics. The authors name this mechanism the Trigger mechanism because coordination of one monomer triggers rapid insertion of the other. Another effect these authors postulate that could lead to the comonomer effect is an increase in chain termination immediately after an α-olefin has inserted, yielding the thermodynamically more favored vinylene end group compared to the vinylidene end group generated from elimination with propylene as the terminal monomer. While the rate of

initiation and early chain growth is faster than the average propagation rate this has the effect of lowering molecular weight and raising productivity.

While much is known about the comonomer effect in ethylene copolymerization with short chain α olefins no mechanism has been sufficient to explain the effect broadly across multiple experimental conditions. While physical effects such as the lowered crystallinity of copolymers relative to PE makes a good explanation for heterogeneous catalysis it doesn't inform why the effect is still seen when polymerization happens entirely in solution state. Additionally, mechanisms like the Trigger effect aren't widely accepted because it does not require a large amount of α olefin to make its way into the polymer for enhanced productivity to been seen.

In this work a further understanding of the comonomer effect is had through careful study of polymerization that begins as a homogenous solution and ceases when the growing polymer falls out of solution, and 1-hexene's effect on this process. In addition polymers of very high 1-hexene are studied in completely conditions where the polymer remains soluble and the effect of a comonomer insertion into the growing polymer chain is measured.

CHAPTER II. Observations of the Comonomer Effect and Possible Mechanisms

A. Generation of Polymer Gels

To evaluate possible mechanisms for the comonomer effect an industrially relevant catalyst[18] (Scheme 2.1) was chosen that has a simple synthesis and excellent stability without compromising activity. Importantly this catalyst does not undergo thermal isomerization or have a metal-carbon bond that a monomer could insert into and change the ligand framework ensuring that the catalyst remains single site during the reaction. It is also known to be able to produce ultra-high molecular weight (>1,000,000 g mol^{-1}) PE due to slow chain termination.[18] Under the temperature and pressure of ethylene utilized in this work high molecular weight PE (100,000 – 300,000 g mol^{-1}) was obtained without any ultra-high molecular weight polymer.

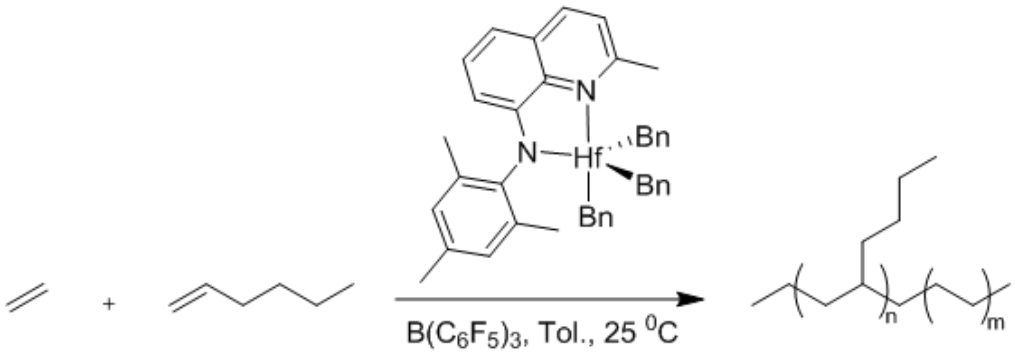

Scheme 2.1 HDPE/LLDPE production afforded by a single site hafnium catalyst in the presence of tris(pentafluorophenyl)borane activator.

Experimental Methods

All manipulations were performed in an argon filled glovebox or by using standard Schlenk techniques under an ethylene atmosphere. Ethylene (99.9999% purity), purchased from Praxair, was filtered through an Oxiclear purifier (RGP-R1-500) before use. Toluene was degassed and purified with a solvent purification system (Pure Process Technology Inc.) and stored over activated molecular sieves prior to use. $Hf(Bn)_4$ was purchased from Strem. All other reagents were purchased from chemical vendors (Sigma, Thermo-Fischer, and VWR International) and used as received. The precatalyst was synthesized from $Hf(Bn)_4$, 2-methylquinolin-8-amine, and 2-bromomesitylene using literature procedures[18] (Scheme 2.2) and characterized by ^1H NMR.

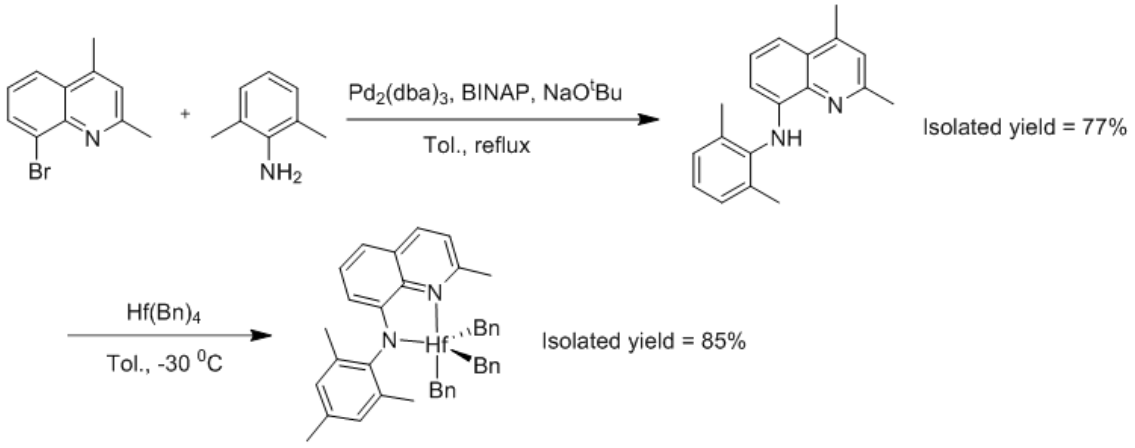

Scheme 2.2 Synthesis of tribenzyl-N-mesityl-2-methylquinolin-8-amine hafnium (IV) precatalyst.

^1H NMR was collected on Agilent 400-MR spectrometer at 25 °C. Quantitative ^{13}C NMR was collected on a Bruker 500B using approx. 50 mg of polymer, 1,2,4 trichlorobenzene, C_6D_6 to lock, and 5 mg of chromium(III) acetylacetonate as a relaxation

agent at 80 °C. For copolymers with low 1-hexene incorporation the peak at 38.1 ppm in the ^{13}C NMR spectrum, corresponding to a -CHR-, was primarily used to estimate hexene content in the copolymer.

Molecular weights (M_n and M_w) and molecular weight distributions ($Đ = M_w/M_n$) of polymers were determined by gel permeation chromatography (GPC). Analyses were performed using an Agilent PL-GPC-220 equipped with a refractive index (RI) detector. The column set (three Agilent PL-Gel Mixed B columns and one PL-Gel Mixed B guard column) was operated with 1,2,4-trichlorobenzene containing 0.01 wt.% 3,5-di-tert-butyl-4-hydroxytoluene (BHT) at a flow rate of 1.0 mL/min at 150 °C. The samples were prepared in 1,2,4-trichlorobenzene (TCB) with BHT at a concentration of 1.0 mg/mL unless otherwise stated and heated at 150 °C for at least 1 hour prior to injection. GPC data calibration was done with monomodal polyethylene standards from Agilent and Polymer Standards Service, Inc.

For a typical polymerization 25 μmol (18.8 mg) of precatalyst was added to 20 mL of dry toluene and transferred to a Schlenk flask, removed from the dry box, and placed on a Schlenk line equipped with a vacuum line and ethylene feed. The argon atmosphere was removed by piercing the septum with a needle under excess ethylene pressure to purge the flask. After 15 minutes of equilibration with the gas phase ethylene the reaction is started by injecting activator solution, 27.5 μmol $B(ArF_5)_3$ (15 mg) in 5 mL of toluene, via needle. At this point the orange precatalyst solution turns to dark red, indicating the catalyst has been activated. Typically, if 1-hexene is present, it is introduced in the activator solution. In either case the ethylene pressure in the atmosphere during the reaction is maintained at 1 bar. The polymerization reaction is quenched by addition of 1 mL of deuterated methanol (MeOD)

causing the dark red color to change to yellow. After being quenched, the reaction mixture is poured into 200 mL of 10% (v/v) HCl/MeOH and stirred overnight to remove quenched catalyst from the polymer. Isolated polymer is white or pale yellow in color and filtered from solution under vacuum and dried at 120 °C for two hours.

Results

The mass of polymer after polymerization for 10 minutes under various 1-hexene concentrations (0-100 mM) and incorporation of 1-hexene in the polymer are summarized in Figure 2.1. Productivity and mass percentage of ethylene in the polymers is shown in Table 2.1. These results are consistent with a comonomer effect because they show a 7-fold increase in total polymer mass while incorporation of 1-hexene remains low (< 10 % by weight). Table 2.1 illustrates how the activity of the catalyst towards both ethylene and 1-hexene is enhanced, in the case of ethylene from 0.19 mol g_{cat}^{-1} h^{-1} to 1.5 mol g_{cat}^{-1} h^{-1}. This data illustrates a threshold in added 1-hexene at which the effect becomes pronounced, below 50 mg (25 mM) of added 1-hexene does not increase productivity in a significant way. This effect quickly falls off, as adding 4 times the 1-hexene (100 mM) only increases productivity moderately, about 30%. An interesting observation is that incorporation of 1-hexene comonomer is linear with respect to 1-hexene incorporation, meaning the excess polymer formed must be because of enhanced reactivity towards ethylene rather than just increased polymerization of 1-hexene.

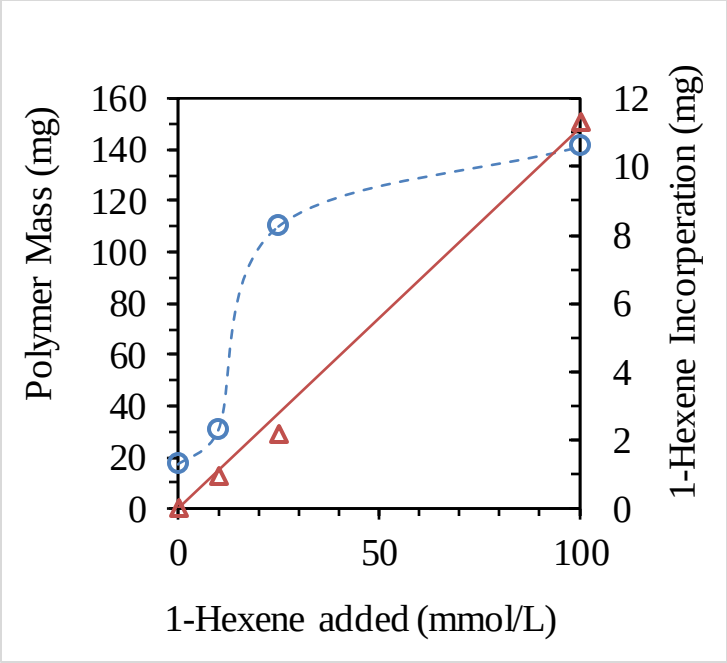

Figure 2.1 Productivity vs added 1-hexene (blue) and mass fraction of hexene in the resulting polymer (red). Blue line is a guide to the eye, red line is a linear best fit (R^2 = 0.997). Conditions: 25 µmol of Hf catalyst with 27.5 µmol $B(ArF_5)_3$ in 25 mL of toluene with 1 bar ethylene pressure. 1-hexene content was determined from Triad analysis of ^{13}C NMR[19]

Table 2.1 Activity and Monomer Content of Polymers produced with Varied 1-hexene

Added 1-hexene/ mg	Isolated polymer/ mg	PE content by % weight	Activity (mol/g_{cat} h)	
			Ethylene	1-hexene
0	17	100	0.19	-
21	31	97	0.34	0.38×10^{-2}
53	110	98	1.2	0.83×10^{-2}
210	141	92	1.5	4.2×10^{-2}

Triad analysis[19] by quantitative ^{13}C NMR was performed and found, for example, that the 141 mg co-polymer produced in the presence of 1-hexene (210 mg) is largely ethylene with only 12 mg of 1-hexene incorporated in the copolymer. Triad analysis is a way of interpreting the complex ^{13}C NMR of copolymers by considering smaller units composed of a monomer and its two nearest neighbors on the polymer chain. For example, the peak in the ^{13}C NMR corresponding to a tertiary carbon surrounded by methylene carbons would be the triad EHE, and it will shift at 38.1 ppm which is distinguishable from a tertiary carbon when one or two neighbors in the beta position is also tertiary (EHH and HHH respectively, shift at 35.8 ppm and 33.5 ppm respectively). For the work described in Chapter II triads were used exclusively to analyze copolymers for total 1-hexene incorporation (mol %), in Chapter III triads are explained in more detail as they are used to extract kinetic information. One can convert between mol % hexene and mass % hexene by using the following formula: M_h/M_t * 100% = mass percent hexene = 3/(3+x). Where M_h is the mass of 1-hexene, M_t is the total mass of polymer, and x is the mol ratio of ethylene to hexene. As an example, for the data in Table 2.1, Entry 2 (Figure 2.2) the triad analysis gives 1.0 % mol hexene or 99 mols of ethylene for every 1 mol of hexene. The mass percent of hexene for this sample is 3/(3+99) = 2.9%, for low hexene incorporation the approximation, mass % ≈ 3*mol %, works well.

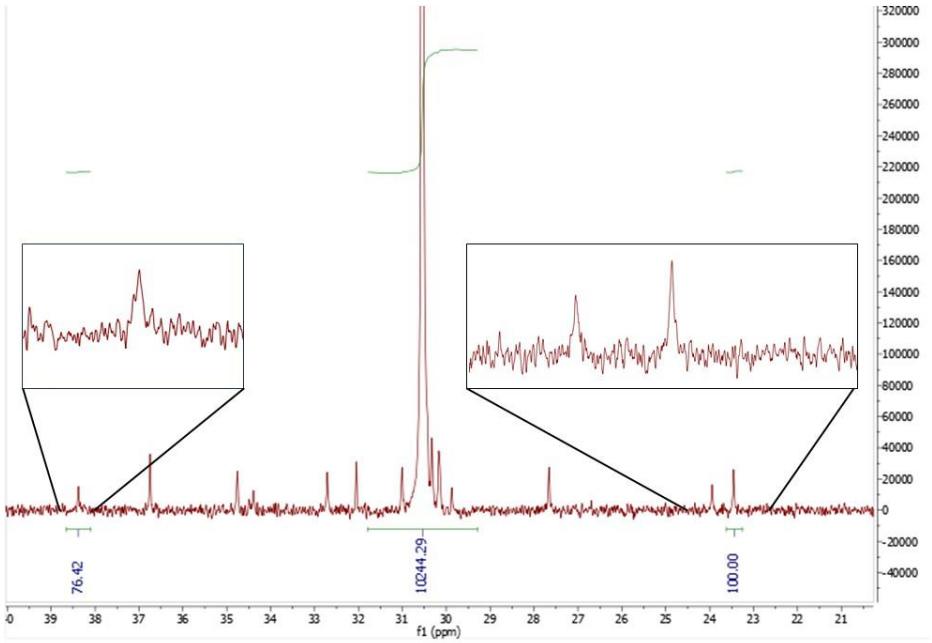

Figure 2.2 ^{13}C NMR of ethylene/1-hexene copolymer synthesized from 25 μmol of Hf catalyst with 27.5 μmol $B(ArF_5)_3$ in 25 mL of toluene with 21 mg of 1-hexene and 1 bar ethylene pressure.

In addition to the amount of polymer isolated, the appearance of the polymer is notably different in the case of the PE homopolymerization versus copolymerization in the presence of 1-hexene (Figure 2.3), specifically the PE polymer forms a single blob (that typically wraps around the stir bar) whereas the copolymer remains a suspension of many particles of varying size. PE (Table 2.1, Entry 1) was isolated as a physical gel, and despite toluene being an anti-solvent for PE, the polymer gel was > 90% solvent by mass. In contrast, the copolymer (Table 2.1, Entry 4) with 8% (wt.) 1-hexene was 67% solvent. The striking contrast between the two polymers is shown in Figure 2.3. The amount of solvent trapped by the polymer in Entry 1 is approximately 6,500 toluene molecules per polymer chain, or a 3:1 ratio of toluene trapped to ethylene consumed. In contrast, Entry 4 only

trapped 200 toluene molecules per polymer chain on average, which is a 1:3 ratio of toluene trapped to ethylene consumed, roughly an order of magnitude less. These differences in the polymer remain after drying; the PE forms large chunks that are very light, indicating that the material is mostly empty space where solvent was once trapped, while the copolymer is dried to a free-flowing powder.

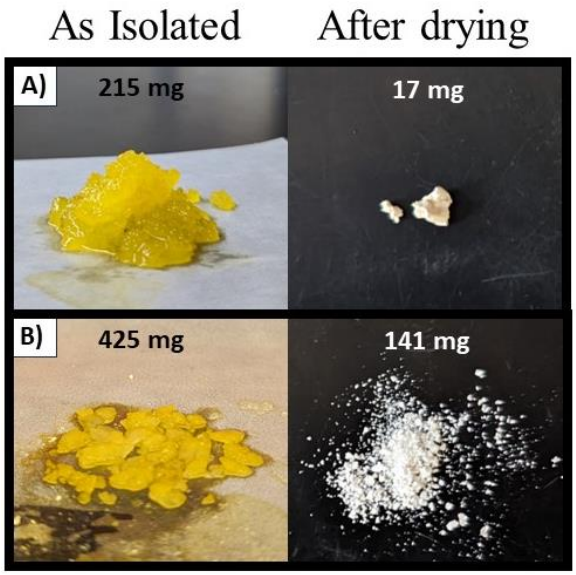

Figure 2.3 PE (top, A) and copolymer (bottom, B) shown as isolated from reaction mixture immediately after quenching (left), the yellow color is due to the quenched catalyst. After the polymer has been isolated from quenched catalyst and dried (right) the mass decreases significantly. Polymer particle size varies between samples, each picture is roughly 1 inch x 1 inch.

To confirm that the formation of large polymer gels in situ were shutting down the reaction a batch was prepared identically to Table 1, entry 1 however it was quenched at 2 minutes (when the gel was first formed) instead of at 10 minutes. That batch of polymer

yielded 14 mg which is very comparable to the 17 mg of polymer when given the full 10 minutes of reaction time.

In addition to the differences between homopolymerization of PE and copolymerization observed during the reaction; high temp GPC revealed very different molecular weight (M_w) curves for the two polymers (Figure 2.4). The PE from ethylene solution without added 1-hexene has a high molecular weight M_w = 170,000 g mol^{-1} and a Đ = 3.2 while the E/H copolymer has M_w = 25,000 g mol^{-1} and Đ = 1.7. The E/H copolymer gives a bimodal distribution with a smaller contribution from a peak at M_w = 300,000 g mol^{-1}, which is assigned to a PE product that is analogous to that produced with ethylene alone. In other words, addition of 1-hexene suppressed the production of the high molecular weight PE but did not eliminate it entirely. Nevertheless, the majority (80%) of the copolymer produced in presence of 1-hexene is the lower molecular weight copolymer that is largely ethylene in composition. Because the copolymer was able to hold onto a large amount of solvent (70%) but significantly less than the PE the solvent rich polymer is attributed to the high molecular weight fraction. By dividing the mass of the polymer by the M_n (54,000 g mol^{-1} and 16,000 g mol^{-1} for PE and copolymer respectively) and normalizing with the total amount of catalyst used (25 μmol) it is found that only 1% of the catalyst is active in homopolymerization of PE while the copolymerization proceeded with 35% of the catalyst active. This calculation assumes that the rate of termination is negligible over 10 minutes, consistent with the absence of vinyl or vinylidene peaks observable in ^{1}H NMR.

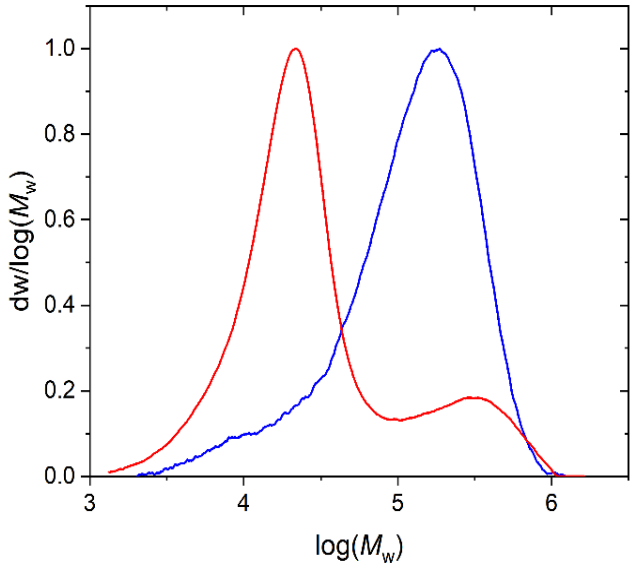

Figure 2.4 Molecular weight (Mw) distributions run on GPC in 1,2,4 trichlorobenzene at 150 ℃ using RI detection with a PE calibration. Polymers synthesized from 1 mM Hf catalyst in 25 mL of saturated toluene in 10 minutes, 210 mg of 1-hexene added to make copolymer.

B. Effects of Limiting Initial Ethylene

It is surmised that if the initial ethylene concentration and hence the monomer-to-active site ratio is reduced, then the growth of the high molecular weight PE would be suppressed, which would in turn prevent the physical gel from forming and more catalytic sites would initiate. In other words, it would create the 'comonomer effect' in the absence of comonomer by controlling ethylene concentration at the beginning of the polymerization reaction.

To test this hypothesis, a reaction was conducted where ethylene was initially in the head space rather than saturating the toluene solution and the stirring was turned on only after pre-catalyst activation. Under the experimental conditions used the diffusion of ethylene

into solution without stirring is known to be slow compared to the catalyst activation/initiation rate, however once strong stirring disturbs the solution surface ethylene diffuses much more readily. The results are summarized in Figure 2.5 and Table 2.2.

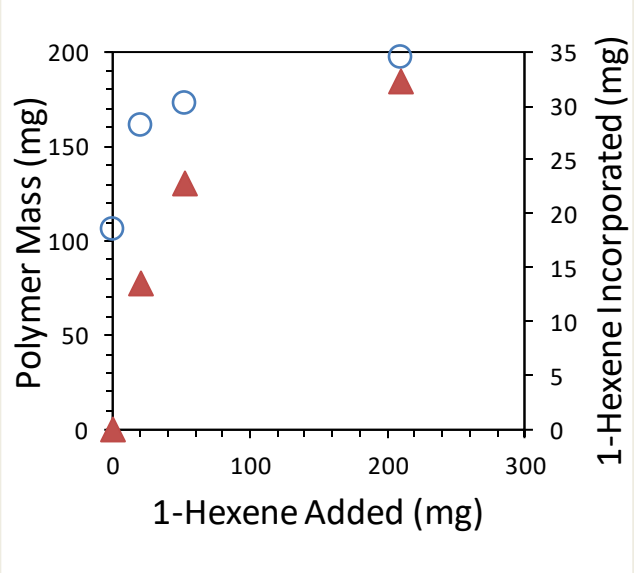

Figure 2.5 Polymer produced (mg) from 1 mM Hf catalyst in 25 mL of toluene in 10 minutes (blue circles) and milligrams of 1-hexene incorporated in that polymer (red triangles). Toluene initially had no ethylene dissolved but at time = 0 rapid stirring allowed ethylene to dissolve from the gas phase. 1-hexene fraction was determined from ^{13}CNMR

Table 2.2 Activity and Monomer Content of Polymers produced with Varied 1-hexene in Ethylene Unsaturated Toluene

Added 1-hexene (mg)	Isolated polymer (mg)	PE content (mass %)	Activity (mol/g_{cat} h)	
			Ethylene	1-hexene
0	105	100	1.2	-
21	121	99	1.4	0.15×10^{-2}
53	161	92	1.7	5.1×10^{-2}

210	197	84	1.9	12 x 10^{-2}

The most striking result from the experiments with unsaturated ethylene is the case of homopolymerization, the amount of polymer produced (105 mg) is essentially the same as was produced in the case with saturated ethylene and 50 mg of 1-hexene (110 mg). This is due to the polymerization proceeding in a similar way, ie many active sites (50% based on a M_n = 8,600 g mol^{-1}) producing small polymer particles suspended in solution instead of one large gel that inhibits monomer mobility. As expected, the M_w of the polymers from unsaturated initial conditions is comparable to the copolymer, with an average of 33,000 g mol^{-1} (Figure 2.6). The polymers obtained from reaction with ethylene initially present only in the gas phase were always very low in solvent incorporation (10%) which is expected if it is only the >100,000 g mol^{-1} polymer that entraps a large amount of solvent.

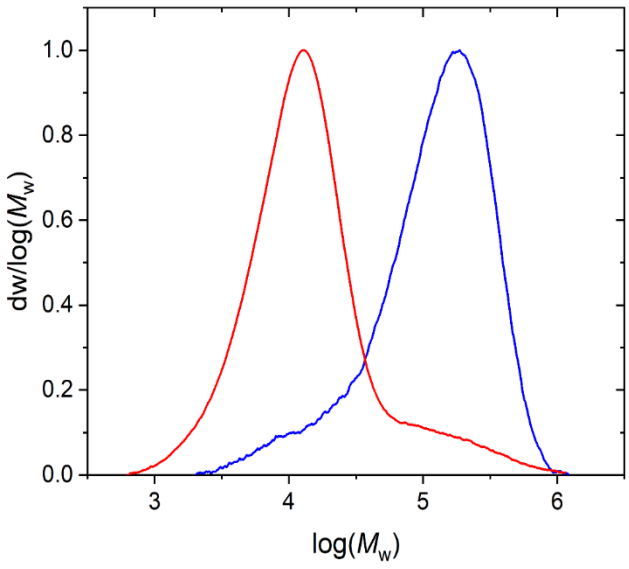

Figure 2.6 Molecular weight (M_w) distributions of polymers from reaction with a saturated ethylene solution (blue) and with an unsaturated solution (red) with ethylene initially only in the headspace obtained by GPC in 1,2,4 trichlorobenzene at 150 °C using RI detection with a

PE calibration. Polymers synthesized from 1 mM Hf catalyst in 25 mL of toluene in 10 minutes.

C. Effects of Pre-activating Catalyst

If the growth of the high molecular weight PE could be suppressed by lowering ethylene concentration in the first few moments of reaction perhaps if all the catalyst was active initially the lowered ethylene to active site ratio would produce the same effect. To test this hypothesis precatalyst and activator were mixed 5, 30, and 60 minutes prior to the reaction and injected into a solution of toluene saturated with ethylene. In the case of homopolymerization this led to a five-fold increase in polymer produced (90 mg PE product in 10 min) as compared to the standard case (Entry 1 in Table 1). The effect was already observed at 5 min mixing time, where 30 and 60 min mixing times produced the same result within experimental scatter (± 4 mg). Interestingly the molecular weight of the polymer was bimodal (Figure 2.7), like the case with 1-hexene added to a saturated ethylene solution; however, there are roughly equal amounts of high and low molecular weight polymer instead of a basis towards the low molecular weight. Significantly less solvent (15 %) was trapped by the growing polymer chains in this case compared to polymerization with in-situ activation (90 %). In contrast no significant difference was seen between copolymer reacted with pre-activated catalyst (132 mg) and without (110 mg).

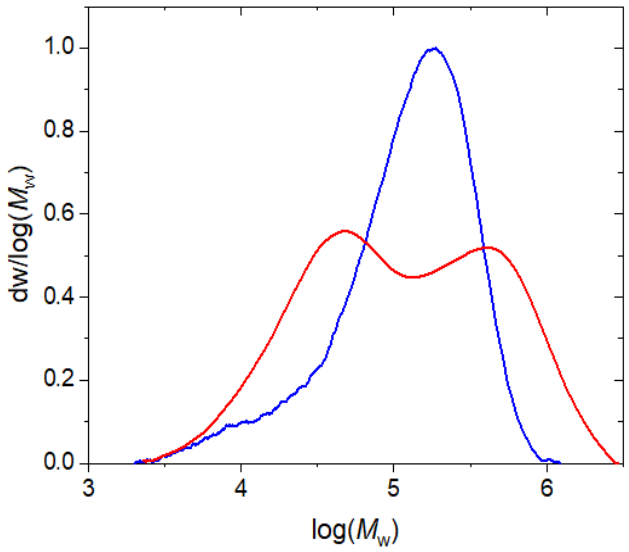

Figure 2.7 Molecular weight (M_w) distributions of polyethylene synthesized from catalyst activated 5 minutes prior (red) and catalyst without Preactivation (blue) obtained by GPC in 1,2,4 trichlorobenzene at 150 °C using RI detection with a PE calibration. Polymers synthesized from 1 mM Hf catalyst in 25 mL of toluene in 10 minutes.

D. Discussion

A drastic comonomer effect was observed where presence of 1-hexene at the concentration of 50 mM or higher resulted in at least 6-fold increase in the mass of the polymer produced as compared to the homopolymerization under the same conditions. The copolymer is 98% ethylene by weight indicating that the mass increase is not due to 1-hexene incorporation. The threshold-like shape of the dependence of the polymer mass on the concentration of 1-hexene (Figure 2.1) rules out a chemical explanation for the comonomer effect; if the 1-hexene were chemically modifying the active site a linear dependence on the 1-hexene concentration would have been observed. Critical to understanding the comonomer effect is the observation that a physical gel is formed in the homopolymerization but not

copolymerization case. The gel is assumed to be responsible for the entrapment of the large amount of solvent. The solvent is not simply wetting the outside of polymer particles because under vacuum it is not fully removed even after 24 hours at room temperature. To remove solvent from the polymer heating in a vacuum oven for 2 hr at 120 °C was required. Note that the polymers' melting temperature (T_m) was 130 ± 1 °C as determined by differential scanning calorimetry (DSC) (Figure 2.8).

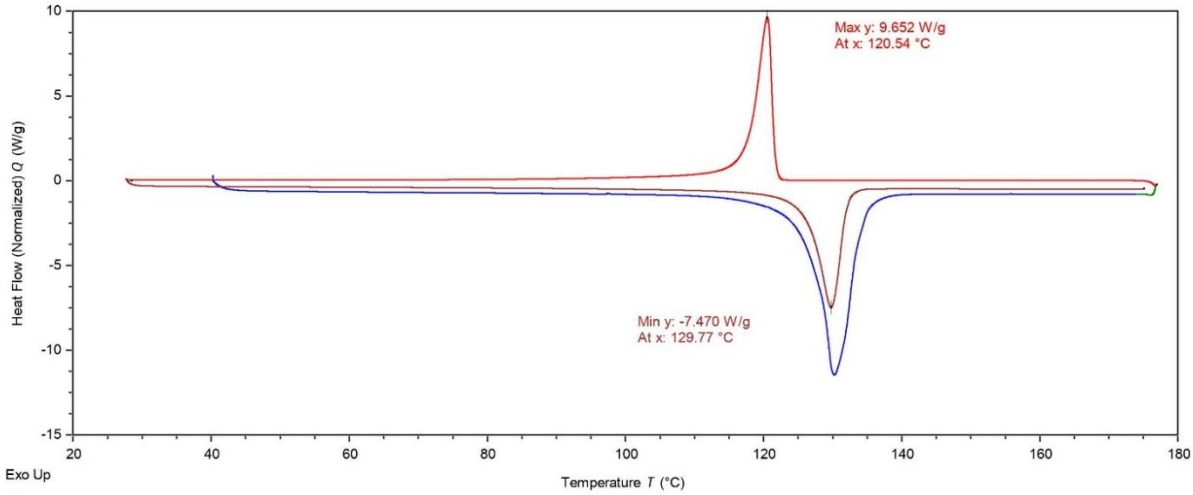

Figure 2.8 DSC of polyethylene synthesized from 1 mM Hf catalyst in 25 mL of toluene in 10 minutes. A 5 mg sample was sealed in a TZero aluminum pan and heated to 177 °C at a rate of 20 °C/min (blue trace) and held at 177 °C for 20 minutes to anneal (green trace). Samples were then cooled at a rate of 10 °C/min (red trace) until they reached 23 °C. Finally, samples were heated to 177 °C at a rate of 10 °C/min (dark red trace).

This implies that some degree of chain mobility is required for the toluene to be able to migrate to the outside of the polymer. When fully dried the polymer isolated from the gel morphology becomes a highly porous light weight solid. In contrast, the polymer isolated from the suspension that is low molecular weight PE and low molecular weight ethylene/1-

hexene copolymer is a fine powder. Interestingly, high molecular weight is a necessary but not sufficient condition for forming a physical gel and trapping large amount of solvent. In the case of the ethylene homopolymerization by the pre-activated catalyst even though there is a significant fraction of high molecular weight polymer the solvent entrapment is low. This shows that the kinetics of polymer growth are crucial for physical gel formation. The difference between the standard and the pre-activated PE homopolymerization experiments is that the monomer-to-active site ratio is significantly higher in the former case. As a result, one speculates, the growth is so explosive in the former case that the chains become entangled before they have a chance to collapse on their respective active sites thereby forming a network structure. In the latter case there are many more active sites where each grows a chain at a slower rate; hence, each chain has the time to find its thermodynamically favored state where it falls into an amorphous globular conformation in the poor solvent. This results in a dense and nearly solvent free polymer particle that does not form a physical gel although it continues to grow, reaching high molecular weight by the end of the reaction. The solvent trapping physical gel is in a thermodynamically unfavorable state at room temperature, which it is unable to escape until heated to near its T_m at which point the polymer chains have enough energy to rearrange and release the solvent. The mechanism of physical gel formation is illustrated in Figure 2.9; specifically, during copolymerization (left) the polymer chains grow slowly and steadily over the course of the reaction. In contrast, ethylene homopolymerization (right) proceeds quickly in the initial stage where the physical gel is formed that snares solvent as well as the active and yet uninitiated catalyst. At this point the catalyst is no longer accessible to monomer and the reaction effectively ceases.

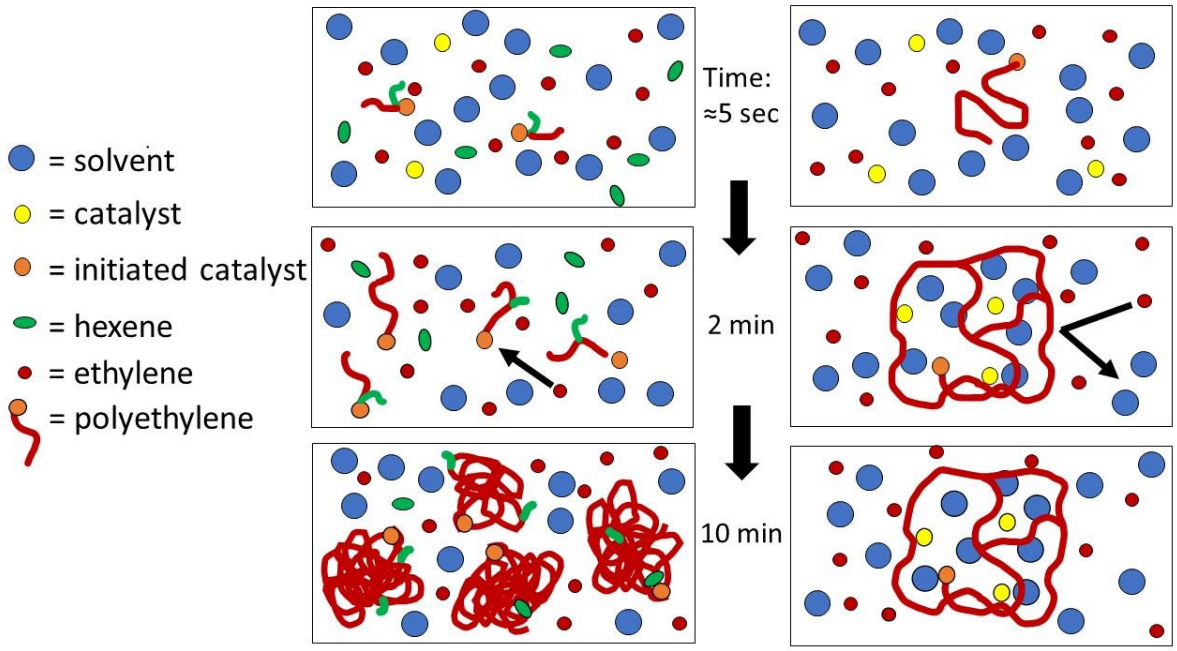

Figure 2.9 Polymer growth under different conditions leads to either a high or low amount of solvent entrapped. In the case with 1-hexene (left) slow growth traps little solvent and polymerization continues. In the homopolymerization case (right) the rapid growth traps the reaction mixture and prevents the diffusion of ethylene to the active site.

E. Conclusion

Summarizing, due to slow initiation in the beginning of the reaction the monomer-to-active site ratio is extremely high where the following course of the reaction diverges into two drastically different scenarios depending on whether it is a homopolymerization of ethylene or a copolymerization with enough 1-hexene present. Under the first scenario a few PE chains rapidly grow to high molecular weight, entangle, and form a physical gel which traps catalyst and large amount of solvent preventing monomer access and effectively stopping the reaction. Under the second scenario even though the initial monomer-to-active

site ratio is equally as high, occasional insertion of 1-hexene slows down the growth of the polymer chains so that the molecular weight is almost an order-of-magnitude lower, and the physical gel is not formed. As a result, more precatalyst has the time to become initiated; the monomer-to-active site ratio decreases, and the polymerization proceeds smoothly until manually quenched producing eight-fold more polymer than in the first scenario. These scenarios account for the entirety of observations, including the molecular weight of the polymer and the amount of trapped solvent in each case. The mechanism is validated in a series of additional experiments aimed at proving that it is the initiation step that plays the key role. In the first experiment named the 'unsaturated ethylene experiment', which was a homopolymerization of ethylene, the initial monomer-to-active site ratio was reduced as compared to the standard case because prior to the start of the reaction the ethylene was only in the headspace rather than in the solution. The unsaturated ethylene experiment produced a five times higher yield of lower molecular weight PE (M_w of 33,000 g mol^{-1} as opposed to 150,000 g mol^{-1} obtained in the standard i.e., saturated ethylene experiment under the same conditions) that trapped little solvent. Thus, the unsaturated ethylene experiment reproduced the comonomer effect without addition of a comonomer. In a second validation experiment the initial monomer-to-active site ratio was reduced as compared to the standard case using a pre-activated catalyst. In case of the homopolymerization of ethylene use of pre-activated catalyst resulted in a five-fold increase in the polymer yield as compared to the standard case; also, despite a significant fraction of high molecular weight chains detected in the product no solvent entrapment was observed. In contrast, when the pre-activated catalyst was used in copolymerization with 1-hexene, no discernable change as compared to the standard case occurred.

CHAPTER III. Deriving Multiple Rate Constants in Copolymerization

A. Introduction

Previously, our group had studied 1-hexene polymerization by single-site Ti, Zr, and Hf–amine bis(phenolate) catalysts activated by $B(C_6F_5)_3$ (BCF)[11,19,20,21] and demonstrated that careful measurement of active sites, monomer consumption, molecular weight distribution, and analysis of terminal alkenes can form the basis of a kinetic model capable of predicting elementary rate constants for the polymerization of 1-hexene. Herein, we extend that analysis to an ethylene/1-hexene copolymerization system which adds complexity in end group analysis (Scheme 3.1) and the number of possible ways the two monomers could get consumed by the reaction (Scheme 3.2).

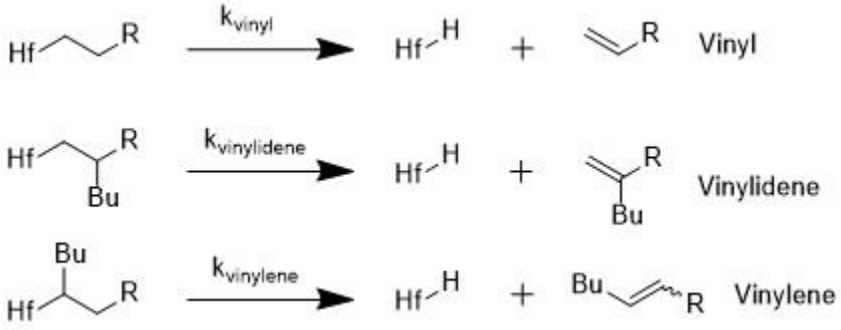

Scheme 3.1 All possible chain termination reactions in the copolymerization of ethylene and 1-hexene. Termination following the insertion of ethylene (top) yields vinyl end groups, termination following the 1,2 insertion of 1-hexene (middle) yields vinylidene end groups, and termination following 2,1 misinsertion of 1-hexene (bottom) yields vinylene end groups.

When modeling the homopolymerization of an α-olefin only one rate constant is needed for propagation, when a second monomer is introduced this will split into a rate of propagation through ethylene, k_E and through hexene, k_H. This could be measured through the consumption of each respective monomer from the total copolymer produced and the ethylene/hexene ratio. However, triad analysis of ^{13}C NMR allows us to go one step forward; because information about a monomer's nearest neighbor is encoded on the polymer chain, we can deconvolute the rate of monomer insertion into a polymer with the previous insertion from ethylene or 1-hexene. Formally we refer to the insertion of monomer X into Y as k_{XY}, for example, insertion of ethylene into hexene is k_{EH} (second from the top in Scheme 3.2). This expands our two rate constants for propagation, k_E and k_H, into four rate constants, k_{EE}, k_{EH}, k_{HE}, and k_{HH} shown in Scheme 3.2.

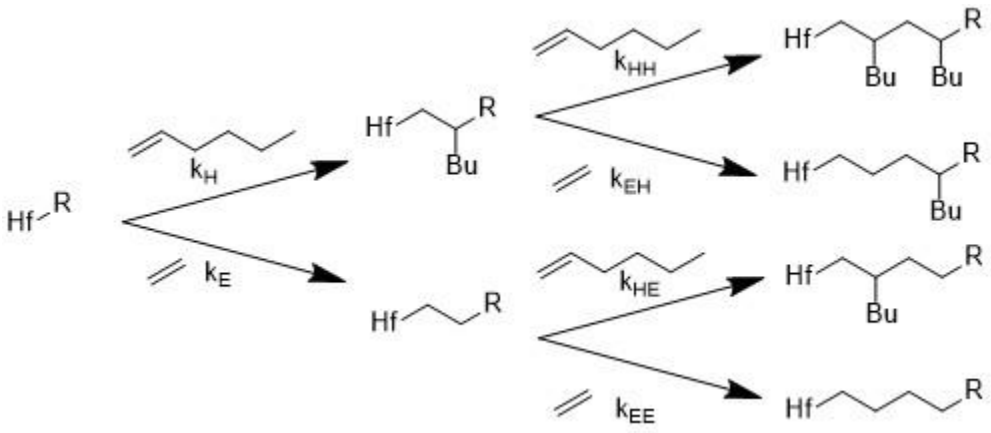

Scheme 3.2 Possible propagation rate constants during the copolymerization of ethylene/1-hexene.

B. Triad Analysis

Triad analysis is a method developed by Seger and Maciel[22] of deconvoluting the peaks found in a ^{13}C NMR of ethylene/1-hexene copolymers. Because the shift of the tertiary

carbon found for every insertion of 1-hexene is dependent on how far it is away from another tertiary carbon a sequence on the polymer chain that looked like -EHE- would be distinguishable from the sequence -EHH- or -HHH-. Seger and Maciel use algebraic combinations of ^{13}C peaks to arrive at the relative concentrations of the six relevant triads: EEE, EEH, EHE, EHH, HEH, and HHH. Once produced these triads do not change, providing a history of inserted monomers, and how those coincide with their neighbors. This allows for more complex kinetic fitting of data, instead of measuring the ethylene consumption to get k_E, measurements of the HEH and EEE triads could be considered independently to detangle k_{EH} from k_{EE}. Unfortunately the same is not true for the EEH triad, because the ^{13}C NMR just sees the nearest neighbors and doesn't know what order they came in the EEH triad is equivalent to the HEE triad. This means that the EEH triad is less discriminating because it could have been formed by either k_{EE} followed by k_{HE} or by k_{EH} followed by k_{EE}.

Because the triads are algebraic combinations of NMR integrations often the percent error cannot be represented accurately by the error in NMR integration. As an example, if we want to calculate the HHH peak following the procedure of Seger and Maciel we use the formula HHH = 2*A + B – G, where A, B, and G refer to integrals of specific regions of the ^{13}CNMR. In one experiment A was 0, B was 90 and G was 100, giving -10. If we assume a 10% error in the NMR integral the value calculated for HHH is -10 ± 10, once this is normalized with the other peaks this corresponds to -0.9 ± 0.9 % which is not useful data to base a model on. However, other triads originate from single peaks, for example the triad EHE = B, in this experiment the B is still 90 so EHE = 90 ± 9 or 7.9 ± 1%. When 1-hexene is in low concentration the HHH peak is most prone to error and when it is in high

concentration the EEE triad is most prone to error because both are low concentrations attempting to be calculated from subtraction of large peaks from each other. To determine the error bars, and whether a given result is significant or not, the standard procedure for propagation of uncertainty is followed. This method requires writing the expression for calculating each triad fraction and computing its partial derivatives with respect to each of the measurement variables. The squares of each derivative are multiplied with the square of each error; then these terms are added before taking the square root, resulting in the propagated error.

The final consideration when using the Seger and Maciel method is α olefin misinsertion. Because of its symmetry ethylene cannot misinsert however 1-hexene can insert normally 1,2 or misinsert 2,1 leaving the polymer attached to the catalyst from a secondary carbon instead of a primary carbon. A misinsertion of hexene could lead to two tertiary carbons side by side instead of spaced by a secondary carbon. A misinserted hexene monomer is called 'J', and in the case of the polymers presented in this study misinsertion was found to be less than 1% of the total hexene inserted which agrees well with previous results[19] on the homopolymerization of 1-hexene by the catalyst used in this study which found that the ratio of propagation through normally insertion and misinsertion, k_p/k_{mis}, was about 100, so misinsertions were not factored into the ^{13}C NMR analysis.

C. Studies of Soluble Polymer

To fully utilize triad analysis to fit rate constants it is important that the polymer stays soluble over the course of the reaction otherwise, the concentration of monomer in the bulk solution will be lower than the concentration of monomer at the active site. For LLDPE the

only way to ensure its solubility is to maintain a temperature at or over its melting point, T_m, which can be achieved on industrial scale by running polymerization at 120-140 °C with thermally stable catalysts[18]. However, on the lab scale it is much easier in practice to lower the T_m to reaction conditions instead by increasing the hexene fraction of the copolymer. Because polyhexene has a T_m well below room temperature we were able to study copolymers with hexene incorporations of 25-85% without observable precipitation (Scheme 3.3).

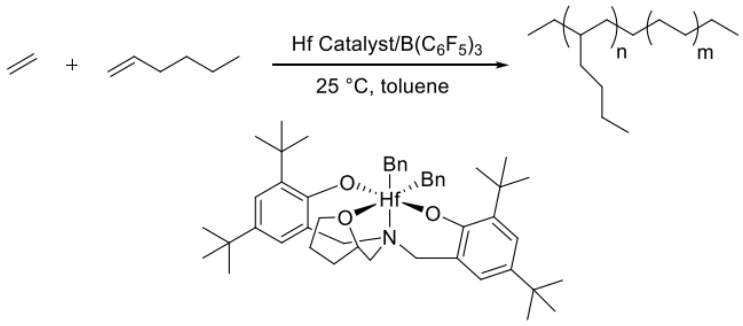

Scheme 3.3 High hexene incorporation copolymers afforded by a single site hafnium catalyst in the presence of tris(pentafluorophenyl)borane activator.

For a typical batch polymerization 30 μmol (26.9 mg) of precatalyst was added to 7 mL of dry toluene with 0.084-2.10 g (0.1 M - 25. M) 1-hexene added and transferred to a Schlenk flask, removed from the dry box, and placed on the Schlenk line. The argon atmosphere was removed by piercing the septum with a needle under excess ethylene to purge the flask. After 15 minutes to equilibrate, the reaction is started by injecting activator solution, 33 μmol $B(ArF_5)_3$ (24 mg) in 3 mL of toluene, via needle. The polymerization reaction is quenched by addition of 1 mL of deuterated methanol (MeOD). Small aliquots of the reaction mixture are removed before the flask is taken from the dry box and after the

reaction is complete. ^{1}H NMR with an internal standard (diphenylmethane) quantifies the 1-hexene concentration before and after the reaction. The results are summarized in Table 3.1

Table 3.1 Copolymers of ethylene and 1-hexene synthesized in batch reaction. Ethylene pressure = 1 bar.

Run	Time	$[Hexene]_i$ (M)	$[Hexene]_f$ (M)	Δ[Hexene] (%)	Hexene incorporation (%)	Yield (mg)
1	30	0.10	0.06	39	25	81
2	30	0.25	0.14	43	46	143
3	10	0.50	0.38	25	78	202
4	30	0.50	0.23	54	72	268
5	90	0.50	0.22	57	68	313
6	10	1.50	1.15	24	86	168
7	30	1.50	0.89	41	85	530
8	90	1.50	0.47	70	81	933
9	90	2.5	2.02	82	85	1,870

D. Preserved Active Sites with High 1-Hexene

In a system with fully soluble polymer quenching the reaction via addition of deuterated methanol (MeOD) in excess to the solution will break the Hf-polymer bond of any catalytic sites still active and replace it with hafnium methoxide and a polymer with a deuterium labeled on one end. In the case of ethylene or 1,2 inserted 1-hexene as the terminal monomer this will yield a primary deuterium and in the case of 2,1 misinserted 1-hexene a secondary deuterium is instead formed (Scheme 3.4). While the two cases that lead

to primary deuterium labels are indistinguishable by ^{2}H NMR, the secondary signal (1.2 ppm) is about 0.4 ppm up-field of the primary signal (0.8 ppm).

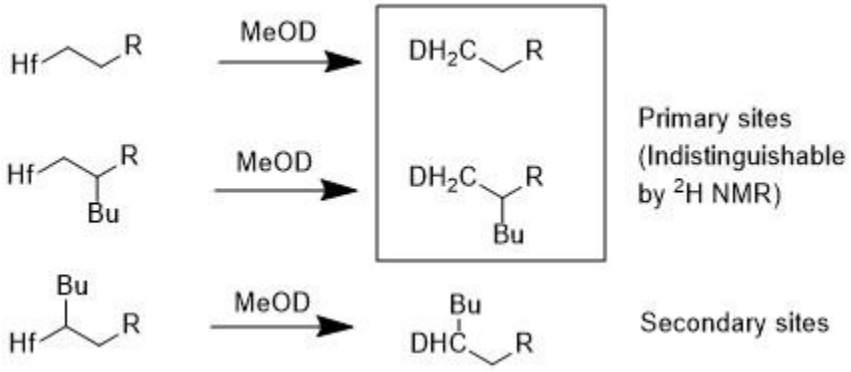

Scheme 3.4 Quenching active catalyst with MeOD to generate 1^{o} and 2^{o} deuterium labeled polymers.

Observations of the primary active sites (Figure 3.1) are consistent with polymerization results, that is they start off at a maximum (approximately 60%) at the earliest time measured, 10 minutes, and drop off near zero as the reaction continues to 90 minutes. The activity of our system is much higher at 10 minutes, and no significant polymerization is seen past 90 minutes, so we concluded that the primary site is the active catalyst. Conversely, secondary sites begin at low concentration and build up over time. Because no polymerization is observed even when secondary sites are 20-40% of the total catalyst in the system we refer to secondary sites as dormant. It is also worth noting that the total active sites (sum of primary and secondary sites) always decrease over time which indicates catalyst deactivation through an unknown mechanism. One possible mechanism of catalyst deactivation is the β-hydride elimination, which leaves the catalyst with a hydride (H^{-}) instead of a benzyl ($C_7H_8^{-}$) ligand. As mentioned previously, the rate of polymerization for BCF activated catalysts is dependent on the distance between the Lewis acid pairs of the

cationic hafnium species and anionic $[B(C_6F_5)_3(C_7H_8)]^-$ with longer Hf-B distances corresponding to higher polymerization rates. The less bulky hydride allows the ion pair to get closer, forming a second species that would also be dormant and would not be picked up by MeOD labeling, releasing HD gas during quenching which would not have escaped detection by ^2H NMR.

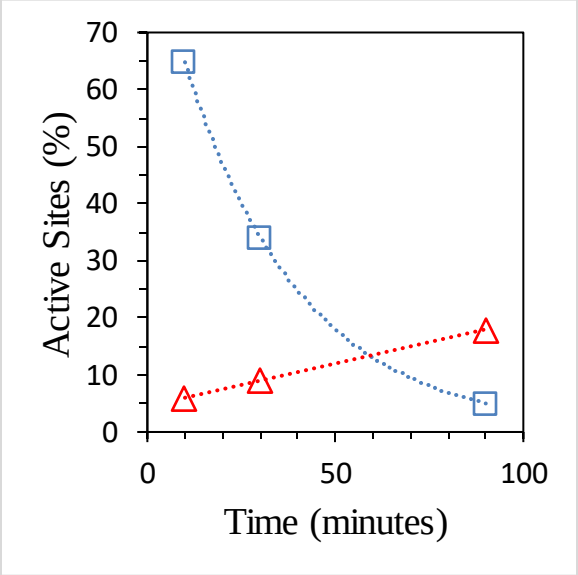

Figure 3.1 Primary (blue square) and secondary (red triangle) active sites in the batch copolymerization of ethylene and 1-hexene shown for batches where initial [1-hexene] = 0.50 mol/L. The lines are intended to guide the eye.

Previous studies[19] of this catalyst in the homopolymerization of 1-hexene also yield secondary active sites, however they remain roughly constant throughout the reaction instead of increasing over time. There exist only two routes for a secondary site to recover, β-hydride elimination or recovery via insertion of another monomer (Figure 3.2). Because β-hydride transfer/elimination is a first order reaction only sensitive to the species and temperature, one wouldn't expect to see any difference between homopolymerization of

hexene and copolymerization. The rate of β-hydride elimination can be easily quantified by ^{1}H NMR. Recovery via insertion of 1-hexene into secondary sites was able to halt the growth of secondary sites at a steady state in hexene homopolymerization[19] however secondary sites continued to grow in copolymerization of ethylene and 1-hexene. Therefore, we conclude that recovery is either not possible or very slow when 1-hexene misinserts into a hafnium-ethylene bond compared to recovery following a misinsertion into a hafnium-hexene bond ($k_{EJH} >> k_{EJE}$ and $k_{HJH} >> k_{HJE}$).

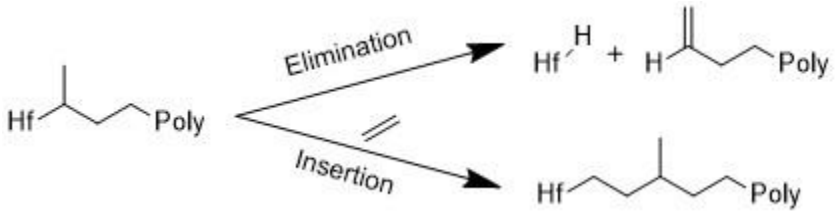

Figure 3.2 Recovery of dormant secondary sites by β-hydride elimination or insertion of another monomer.

Initial hexene concentration has a significant effect on how quickly primary sites decrease, with higher hexene concentrations preserving primary active sites for a longer time than reactions with low initial 1-hexene concentration (Figure 3.3). For example, at the end of 90 minutes when [1-hexene] was 0.50 M the primary active sites were 5% and when [1-hexene] was 1.5 M the primary active sites were 20%. Initial hexene concentration had some effect on secondary sites as well, however the trend is unclear.

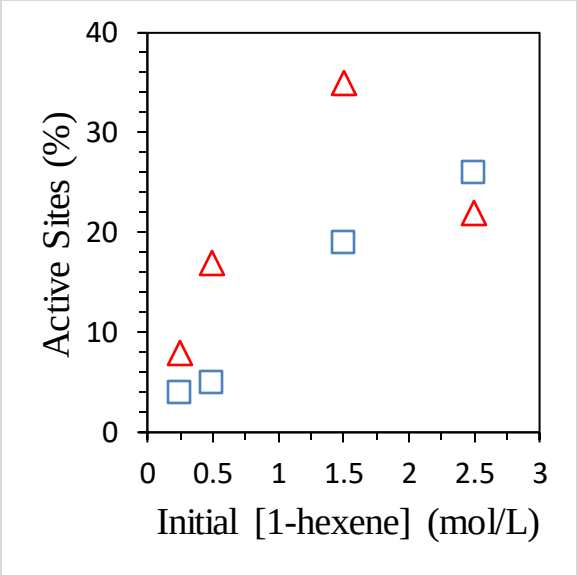

Figure 3.3 Primary (blue square) and secondary (red triangle) active sites after 90 minutes of copolymerization at various initial concentrations of 1-hexene.

E. Modeling Rate Constants

A previous study[11] by this group quantified rate constants from this catalyst in the case of 1-hexene homopolymerization. This is very useful because it means that some rate constants can be set before the model starts adjusting rate constants to fit the data. Specifically, the rate of propagation is k_{HH} = 0.53 $M^{-1}s^{-1}$ and the rate of misinsertion is k_{JH} = 0.0081 $M^{-1}s^{-1}$. The rate of recovery, k_{HJ}, and the rate of misinsertion into a misinserted hexene, k_{JJ}, were both assumed to 0. This is because the species was found to prefer chain termination to recovery with a $k_{vinylene}$ = 0.27 $M^{-1}s^{-1}$. We assume that chain termination leads to an inactive hafnium hydride species. This means that of the nine possible propagation rate constants four have been set and the remaining five are optimized. Similarly, of the three possible chain termination events two have already been set by a previous study and only the termination from ethylene, k_{vinyl}, remains. Vinyl peaks were not observed in ^{1}H NMR spectra

of the studied copolymers so k_{vinyl} was assumed to be 0. The results of the propagation and termination rate constants from optimization of the kinetic model are shown in Table 4.

Table 4. Rate Constants for Ethylene/Hexene Copolymerization

Rate	Rate Constant ($M^{-1}s^{-1}$)	
k_{EE}	0.10 (± 0.02)	Insertion of ethylene into ethylene
k_{HE}	0.05 (± 0.01)	Insertion of hexene into ethylene
k_{JE}	0.0005 (± 0.0002)	Misinsertion of hexene into ethylene
k_{EH}	0.9 (± 0.3)	Insertion of ethylene into hexene
k_{HH}	0.53 (± 0.06)	Insertion of hexene into hexene
k_{JH}	0.0081 (± 0.0002)	Misinsertion of hexene into hexene
k_{vinyl}	0	Chain transfer from ethylene
$k_{vinyldiene}$	0.84 (± 0.03)	Chain transfer from hexene
$k_{vinylene}$	0.27 (± 0.06)	Chain transfer from misinserted hexene

The fits are in good agreement with literature data that suggests that ethylene insertion is always faster than hexene, in this case by a factor of 2 ($k_{EX} \approx 2*k_{HX}$). A more striking result is comparing the insertion of any monomer when the previous monomer was hexene instead of ethylene. If the previous monomer inserted was hexene the next monomer, regardless of identity, would insert an order of magnitude faster ($k_{XH} \approx 10*k_{XE}$). This would satisfy a chemical explanation for the comonomer effect, while the insertion of hexene might be half as fast as ethylene, it speeds up the next insertion by a factor of ten so overall the catalyst is more active.

Interestingly these results were not seen when the copolymerization of ethylene and 1-octene were studied[21] by a different catalyst (Cp_2HfCl_2) activated with MAO. That study

found that the rate of ethylene insertion was about 100 times faster into an ethylene monomer rather than into an octene monomer. Additionally, the k_{OO} insertion of octene after octene had been inserted previously was too small to measure, instead of larger than insertion of α olefin following ethylene in our system. Further study is needed to determine if the difference in kinetic effects of the previous insertion in our work and this study was due to a difference in catalyst or experimental conditions.

F. Conclusion

During copolymerization with high levels of 1-hexene present the amount of 1-hexene at the start of the reaction is critical to how the active sites change over time, with higher hexene concentration leading to more active sites after 90 minutes. In addition, ethylene has a negative effect on the quality of active sites, when ethylene is present dormant secondary sites build up over time rather than recover, leading to trailing off productivity in longer reactions. Given data on hexene homopolymerization as well as copolymerization data with different initial hexene concentrations and reaction durations a comprehensive kinetic model was able to fit the data reasonably well and with the assistance of triad analysis was able to deconvolute k_{EE} from k_{EH}. In other words the model was able to distinguish an ethylene insertion directly after another ethylene from insertion following a hexene, instead of returning a weighted average. This found that having a hexene inserted rather than ethylene would speed up the next insertion, regardless of monomer, by a factor of ten.

CHAPTER IV. Isotopic Labeling of Copolymers

A. Introduction

Deuterated polymers have a long history of study going back about as far as polymers, with the easiest method being H/D exchange of a proton polymer (in this case polypropylene) via D_2 gas and a catalyst.[24] Early material science needed a convenient way to characterize polymers, and without any heavy nuclei in polymers containing only carbon and hydrogen, X-Ray diffraction will have a low signal. However, in neutron diffraction the deuterium atom can scatter much stronger than protium and measurements like crystal lattice structures and cell lengths can be made. In addition this work allowed verification that isotactic (stereo-specific) polypropylene can be converted to the atactic (stereo-random) form by a nickel-kieselguhr catalyst. Before this labeled experiment it was thought that atactic polymer differed from its isotactic form by the degree of chain branching, if this was the case it would have been impossible to form atactic polymer from isotactic polymer with only proton exchange on tertiary carbons.

More recently, X-ray diffraction of deuterated polystyrene was used to study[25] the interaction of the polymer with alumina nanopores. Small angle neutron scattering (SANS) was sensitive enough to confirm that proton polystyrene in the melt phase was able to enter the alumina nanopores, but was unable to determine their configuration. By fully deuterating only a fraction of the polystyrene a sharp contrast between the proton and deuterium polymer was able to be observed that showed polystyrene adopted a linear conformation inside the pores and a globular conformation outside the pores.

Deuterated polymers have also assisted chemists in doing time resolved kinetic studies[26], for example telechelic polymers (polymers with a hydrophobic end group and hydrophilic backbone) are of interest because they will self assemble into micelles in aqueous solution. It was known that the micelles would exchange polymer chains with nearby micelles in solution but not how quickly until time resolved SANS was performed on an aqueous mixture of deuterated and undeuterated telechelic poly(ethylene oxide). These results allowed the researchers to suggest a novel mechanism of exchange that is mediated by the combination of two micelles rather than dissociation of a polymer chain followed by association to a second micelle.

There are many reasons why a chemist would want to study a fully deuterated polymer; this work will focus on efforts to partially deuterate polymers only at specific sites with the end goal of eluding the mechanism of polymer degradation during pyrolysis. Plastic degradation is of particular interest because current production of plastic, 400 million tons annually, greatly exceeds our current recycling of plastic, 50 million tons.[1,27] The majority of plastic waste ends in a landfill, burned for power production, or in the environment. A well-known issue in plastic recycling is that the conditions for reforming plastic into new shapes (high temperature and/or shear stress) will break large M_w chains down, often reducing the material properties of the recycled plastic. Plastic upcycling aims to take advantage of this by further degrading polymer chains until they are better characterized as small molecules instead of macromolecules. If these small molecules have greater value than the plastics used to make them, they are considered upcycled. Similar to how a large family of catalysts are suitable for polyethylene production many catalysts for the degradation of polyethylene at elevated temperatures (200-250 °C) are studied to better understand the chemical mechanism

of plastic degradation,[28-31] including computational methods like DFT.[32] However, studies utilizing different isotopes of hydrogen or carbon to validate mechanisms are lacking in literature to date which is why we choose to target these molecules.

LLDPE primarily contains two distinct environments along the backbone, methylene (-CH_2-) and methylyne (-CHR-). This means that α-olefins that are substituted with an isotopic label in either the 1 or 2 position can directly test how adjusting the kinetic isotope effect on methylene and methylyne carbons (respectively) affects the rate of degradation. In addition, because the resulting pyrolysis oil is a mixture of many different carbon chain length molecules, mass spectrometry (MS) is often used to analyze the post reaction mixture. Using a ^2H label will shift the mass of any molecules derived from those atoms up by one, making them easy to spot in a mass spectrum. It is possible that analysis by mass spectrum of labeled polymers would point towards unique mechanisms, for example if LLDPE was synthesized from ethylene and 1-hexene that was deuterated at the second position MS data would be able to suggest a 1,5 radical transfer scission event (Figure 4.1) if roughly half of the deuterium was found at m/z = 113.13, corresponding to $C_6H_{11}D$. It is thought that 1,5 radical transfer scission is a major contributor to the thermal degradation of polyethylene because of the 5-membered ring confirmation is the most stable way for a carbon chain to interact with itself[33].

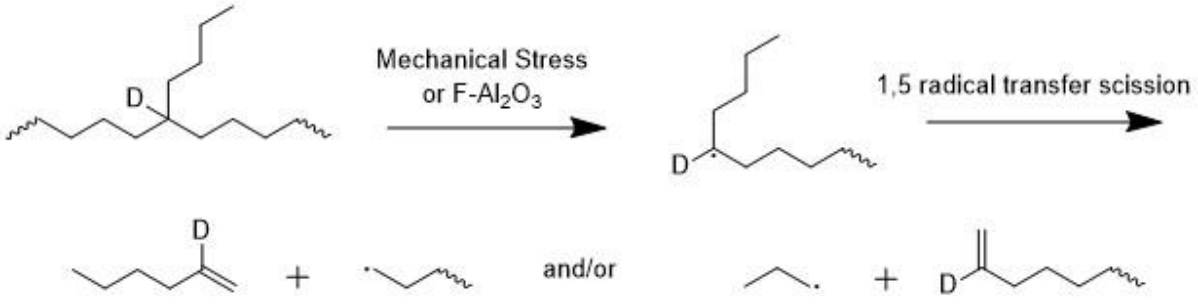

Figure 4.1 First a radical is generated either through hemolytic cleavage of a C-C bond due to mechanical stress on the polymer or through alkyl abstraction by a Lewis acid catalyst. Next radical 1, 5 chain scission can occur which can either reform the starting monomer or generate a saturated hydrocarbon 3 carbons shorter than the original monomer.

Synthesis of Isotopically labeled Monomers

The Wittig reaction pairing carbonyls with phosphonium ylides makes an excellent framework for deuteration because the phosphonium salts (precursors to ylide complexes) will undergo H/D exchange in the presence of a catalytic amount of base[34] (Figure 4.2). Once the Wittig reagent has been tagged with a deuterium the reaction can proceed normally to convert aldehydes into primary alkenes. In the case of labeling the alpha carbon, deuterated methylene Wittig reagents are combined with an aldehyde of one carbon smaller than the desired carbon chain length. For labeling on the β carbon a Wittig reagent with one carbon smaller than the desired chain length is combined with formaldehyde to generate the labeled alkene.

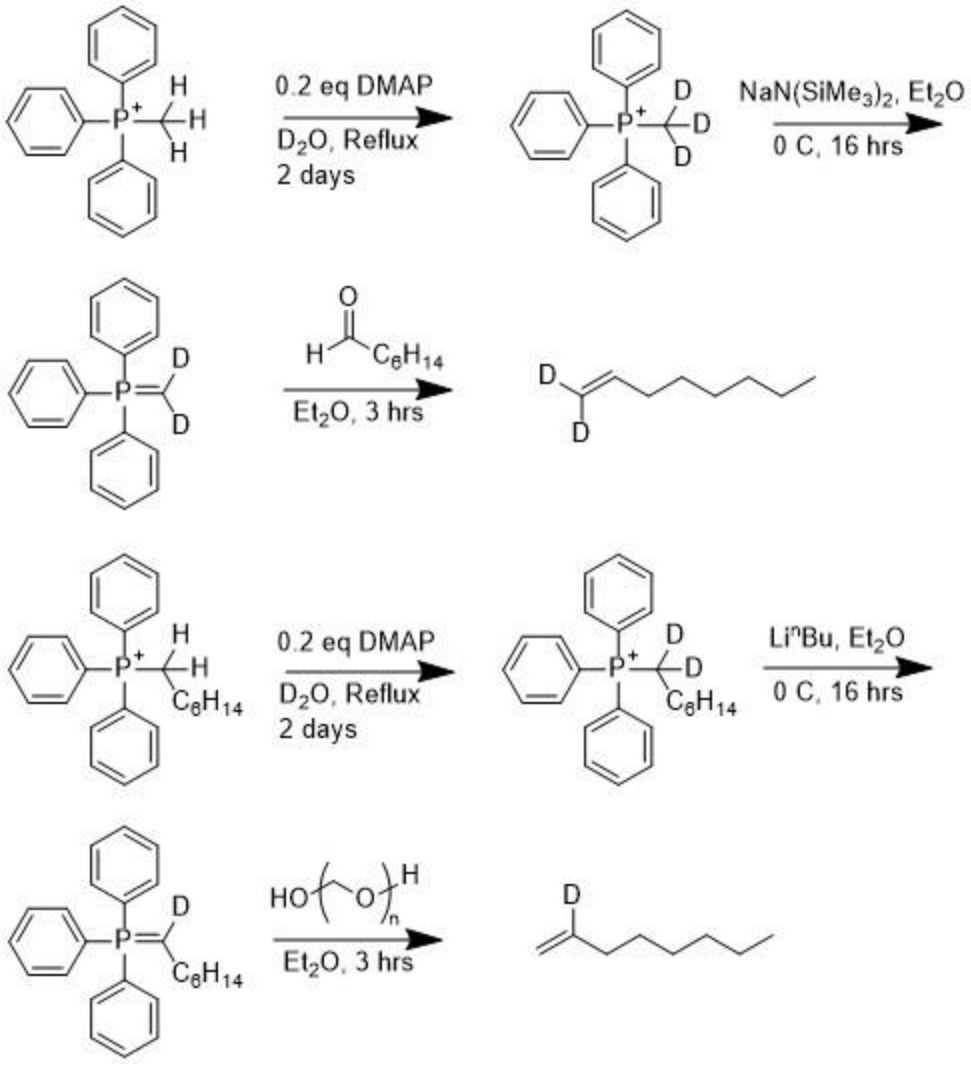

Figure 4.2 Synthesis of 1,1 (^{2}H) 1-octene (top) and 2 (^{2}H) 1-octene (bottom) via H/D exchange of phosphonium salts followed by the Wittig reaction of aldehydes.

Synthesis of [Ph_3P-CH_3]I

A 500 mL 2-neck Schlenk flask equipped with a stir bar was loaded with 39.0 g PPh_3 (149 mmol) and 110 mL of toluene. The flask was sealed, connected to a Schlenk line, cooled in an ice bath, and under N_2 flow, 23.2 g of MeI (164 mmol) was added dropwise to the stirring solution. The flask was sealed, warmed to room temperature, and stirred for 5

days resulting in the formation of a white precipitate. Removal of volatiles under reduced vacuum afforded 59.8 g (98% yield) of a white solid that matched literature values.

^{1}H NMR (400 MHz, 25 °C, CD_2Cl_2): δ 7.88-7.83 (m, 6H), 7.73-7.70 (m, 9H), 3.06 (d, J_{PH} = 13.3 Hz, 3H).

$^{13}C\{^{1}H\}$ NMR (101 MHz, 25 °C, CD_2Cl_2): δ 135.6 (d, J_{PC} = 3.2 Hz), 133.6 (d, J_{PC} = 10.7 Hz), 130.8 (d, J_{PC} = 12.9 Hz), 119.1 (d, J_{PC} = 89.0 Hz), 11.5 (d, J_{PC} = 57.8 Hz).

$^{31}P\{^{1}H\}$ NMR (162 MHz, 25 °C, CD_2Cl_2): δ 21.4.

Synthesis of $[Ph_3P\text{-}CD_3]I$

A 2-neck Schlenk flask equipped with a reflux condenser and stir bar was placed under N_2 atmosphere. The flask was loaded with 22.0 g of $[Ph_3P\text{-}CH_3]I$ (54.4 mmol), 1.33 g of 4-dimethylaminopyridine (DMAP) (10.9 mmol), and 20 mL of D_2O. The heterogeneous suspension was refluxed for 3 days during which the solution became homogeneous. The reaction was allowed to cool to room temperature resulting in the precipitation of a white solid, to which was added 7 mL of 2.0 M HCl to solubilize DMAP. The aqueous solution was extracted with dichloromethane (4 x 20 mL) and dried over anhydrous $MgSO_4$. The volatiles were removed under dynamic vacuum overnight to remove residual water and HCl vapors vacuum to afford 20.7 g of white solid (91% yield, 97 % deuterium incorporation). NMR spectra matched the one obtained for $[Ph_3P\text{-}CH_3]I$ except for the peak at 3.06 ppm was almost completely missing. Deuterium incorporation was calculated by integration of the ^{1}H NMR spectra and the following formula: % D = (15 – (integration at 3.1 ppm) x 5) x 100% when the integration of the benzyl region 7.6-7.9 ppm is set to 15.

^{1}H NMR (500 MHz, 25 °C, CD_2Cl_2): δ 7.85-7.82 (m, 3H), 7.74-7.68 (m, 12H).

^{2}H NMR (77 MHz, 25 °C, CD_2Cl_2): δ 3.06 (br s).

$^{13}C\{^{1}H\}$ NMR (126 MHz, 25 °C, CD_2Cl_2): δ 135.4 (d, J_{PC} = 3.20 Hz), 133.4 (d, J_{PC} = 10.7 Hz), 130.5 (d, J_{PC} = 12.9 Hz), 118.8 (d, J_{PC} = 88.8 Hz), 11.5-9.6 (m).

$^{31}P\{^{1}H\}$ NMR (202 MHz, 25 °C, CD_2Cl_2): δ 21.2.

Synthesis of $Ph_3P{=}CD_2$

To a 500 mL round bottom flask equipped with a stir bar and loaded with 19.9 g of $[Ph_3P\text{-}CD_3]I$ (48.9 mmol) and 200 mL of diethyl ether was added 8.65 g of $NaN(SiMe_3)_2$ (47.2 mmol) as a solid. Immediately, the white heterogeneous solution turned yellow and was stirred for 3 hours, during which an off-white precipitate formed. The yellow solution was filtered through Celite to remove NaI and unreacted $[Ph_3P\text{-}CD_3]I$, and the yellow filtrate was placed under vacuum to remove volatiles to afford 2.95 g (97 % yield) of a yellow solid. The bases $NaNH_2$ and Li^nBu were also explored for deprotonation of the phosphonium salts. $NaNH_2$ resulted in proton exchange with deuterium, although yields were similar deuterium incorporation was low. Li^nBu, which is traditionally used for generation of ylides in situ, gave multiple uncharacterized species ^{31}P NMR that proved difficult to isolate from the desired product. For these reasons $NaN(SiMe_3)_2$ was used as the base for deprotonation of the Wittig species going forward.

^{1}H NMR (500 MHz, 25 °C, C_6D_6): δ 7.74 (dd, J_{HH} = 11.9, J_{HH} = 7.4 Hz, 6H), 7.08-7.01 (m, 9H).

^{2}H NMR (77 MHz, 25 °C, C_6D_6): δ 0.77 (br s).

$^{13}C\{^{1}H\}$ NMR (126 MHz, 25 °C, C_6D_6): δ 135.2 (d, J_{PC} = 84.1 Hz), 132.6 (d, J_{PC} = 9.6 Hz), 130.6 (d, J_{PC} = 3.0 Hz), 128.4 (d, J_{PC} = 11.4 Hz), -4.95 (dp, J_{PC} = 99.8 Hz, J_{DC} = 23.5 Hz).

$^{31}P\{^{1}H\}$ NMR (202 MHz, 25 °C, C_6D_6): δ 20.7.

Synthesis of 1,1-^{2}H-octene

In a glovebox, a 50 mL round bottom flask equipped with a stir bar was loaded with 3.16 g of [$Ph_3P{=}CD_2$] (11.4 mmol), 100 mL of Et_2O, and cooled in a cold well to 0 °C. To the cold, yellow stirring solution was added 1.30 g of heptanal (11.4 mmol) in 7 mL of Et_2O. The solution was allowed to warm to room temperature over the course of 3 hours during which the solution turned pale yellow and a white precipitate formed. The flask was removed from the glovebox, filtered through Celite, and rinsed with pentane. The colorless filtrate was concentrated to afford a colorless oil with a small amount of white precipitate ($OPPh_3$) that was loaded onto a long silica column and flushed with pentane. The pentane fraction was collected and carefully distilled to afford 0.90 g of a colorless liquid (69.2 % yield).

^{1}H NMR (500 MHz, 25 °C, C_6D_6): δ 5.83-5.79 (m, 1H), 2.04 (q, J_{HH} = 7.0 Hz, 2H), 1.40-1.35 (m, 2H), 1.33-1.27 (m, 6H), 0.89 (t, J_{HH} = 6.8 Hz, 3H).

^{2}H NMR (77 MHz, 25 °C, C_6D_6): δ 5.00 (dd, J_{HD} = 5.2, 2.1 Hz, 2H).

$^{13}C\{^{1}H\}$ NMR (126 MHz, 25 °C, C_6D_6): δ 139.2, 113.7 (p, J_{CD} = 23.9 Hz), 33.9, 31.9, 29.1, 29.0, 22.8, 14.2.

Synthesis of [Ph_3P-C_7H_{15}]Br

Under N_2 atmosphere a 500 mL Schlenk flask equipped with a stir bar was loaded with 60.0 g of Ph_3P (229 mmol), 120 mL of toluene, and 40.9 g of 1-bromoheptane (229 mmol). A reflux condenser was attached and the solution refluxed for 4 days during which the formation of a white precipitate was observed. The solution was cooled to room temperature, the white solid was collected on a frit, washed with toluene (3 x 20 mL) and pentane (3 x 20 mL) and dried by removal of volatiles under dynamic vacuum to afford 71.8 g of a white solid (72 % yield).

^{1}H NMR (400 MHz, 25 °C, CD_2Cl_2): δ 7.85-7.73 (m, 15H), 3.56-3.49 (m, 2H), 1.66-1.25 (m, 4H), 1.24-1.21 (m, 6H), 0.85 (t, J_{HH} = 7.6 Hz, 3H).

^{13}C{^{1}H} NMR (MHz, 25 °C, CD_2Cl_2): δ 135.5 (d, J_{PC} = 3.3 Hz), 134.0 (d, J_{PC} = 10.0 Hz), 130.8 (d, J_{PC} = 12.5 Hz), 118.6 (d, J_{PC} = 86.2 Hz), 31.8, 30.9 (d, J_{PC} = 16.0 Hz), 29.1, 23.3 (d, J_{PC} = 49.9 Hz), 22.90, 14.16.

^{31}P{^{1}H} NMR (162 MHz, 25 °C, CD_2Cl_2): δ 23.9.

Synthesis of [Ph_3P-CD_2-C_6H_{13}]Br

A 250 mL Schlenk flask equipped with a stir bar was loaded with 30.0 g of [Ph_3P-C_7H_{15}]Br (67.9 mmol), 1.66 g of DMAP (13.6 mmol), and 20 mL of D_2O. The flask was fitted with a reflux condenser and the heterogeneous reaction mixture refluxed for 3 days under nitrogen atmosphere. The reaction was allowed to cool to room temperature resulting in the precipitation of a white solid, to which was added 11 mL of 0.30 M HCl to solubilize DMAP. The aqueous solution was extracted with dichloromethane (3 × 50 mL) and dried over anhydrous $MgSO_4$. The volatiles were removed under vacuum to afford 28.1 g of a white solid (93 % yield, 95 % deuterium incorporation). Deuterium incorporation was

calculated by integration of the ^{1}H NMR spectra and the following formula: % D = (15 – (integration at 3.5 ppm) x 7.5) x 100% when the integration of the benzyl region 7.6-7.9 ppm is set to 15.

^{1}H NMR (500 MHz, 25 °C, CD_2Cl_2): δ 7.85-7.77 (m, 9H), 7.73-7.69 (m, 6H), 1.65-1.54 (m, 4H), 1.31-1.18 (m, 6H), 0.83 (t, J_{HH} = 6.95, 3H).

^{2}H NMR (77 MHz, 25 °C, CD_2Cl_2): δ 3.55 (br).

$^{13}C\{^{1}H\}$ NMR (126 MHz, 25 °C, CD_2Cl_2): δ 135.4 (d, J_{PC} = 3.0 Hz), 134.0 (d, J_{PC} = 9.9 Hz), 130.8 (d, J_{PC} = 12.5 Hz), 118.5 (d, J_{PC} = 86.0 Hz), 31.7, 30.7 (d, J_{PC} = 15.9 Hz), 29.0 (d, J_{PC} = 1.3 Hz), 22.84, 22.67 (d, J_{PC} = 4.5 Hz), 14.1.

$^{31}P\{^{1}H\}$ NMR (202 MHz, 25 °C, CD_2Cl_2): δ 23.83.

Synthesis of $[Ph_3P{=}CD\text{-}C_6H_{13}]Br$

A 500 mL Schlenk flask equipped with a stir bar was loaded with 15.0 g of $[Ph_3P\text{-}CD_2\text{-}C_6H_{13}]Br$ (33.8 mmol) and 150 mL of Et_2O and cooled to -35 °C in a cold well. The reaction flask was removed from the cold well, placed on a stir plate, and while cold to the stirring solution was added 13.5 mL of 2.5 M Li^{n}Bu (33.8 mmol) dropwise. The solution turned red-orange, warming to room temperature and stirred for an additional 12 hours. The homogeneous solution was placed under vacuum to remove volatiles to afford a sticky red oil. The oil was dissolved in pentane and filtered through Celite to remove solids. The red-orange filtrate was placed under vacuum to remove volatiles and afford 11.9 g (98 % yield) of a red-orange solid.

^{1}H NMR (500 MHz, 25 °C, C_6D_6): δ 7.85-7.50 (m, 6H), 7.09-6.99 (m, 9H), 2.43 (dt, J_{HH} = 14.9, 7.2 Hz, 2H), 1.75 (p, J_{HH} = 7.3 Hz), 1.54 (t, J_{HH} = 7.5 Hz, 2H), 1.37-1.25 (m, 4H), 0.89 (t, J_{HH} = 6.9 Hz, 3H).

^{2}H NMR (77 MHz, 25 °C, C_6D_6): δ 1.06 (br s) .

^{13}C{^{1}H} NMR (126 MHz, 25 °C, C_6D_6): δ 134.2 (d, J_{PC} = 82.7 Hz), 133.0 (d, J_{PC} = 9.2 Hz), 130.5 (d, J_{PC} = 2.7 Hz), 128.4 (d, J_{PC} = 11.2 Hz), 36.8 (d, J_{PC} = 11.8 Hz), 32.5, 29.5, 27.0 (d, J_{PC} = 6.0 Hz), 23.3, 14.5, 11.5 (dt, J_{PC} = 117.1 Hz, J_{DC} = 23.7 Hz).

^{31}P{^{1}H} NMR (202 MHz, 25 °C, C_6D_6): δ 12.8.

Synthesis of 2-^{2}H-1-octene

A 500 mL round bottom flask equipped with a stir bar was loaded with 1.98 g of paraformaldehyde (65.8 mmol formaldehyde eq.) and 150 mL of diethyl ether. To the white, heterogeneous solution was added dropwise the red-orange solution containing 11.9 g of [Ph_3P=CD-C_6H_{13}]Br (32.9 mmol) in 10 mL of Et_2O. The red-orange color disappeared after each drop was added to the paraformaldehyde solution. After complete addition of the ylide, the solution stirred for an additional 12 hours yielding an off-white heterogeneous solution. The flask was removed from the glovebox, filtered through Celite to remove unreacted paraformaldehyde and triphenylphosphine oxide, and rinsed with pentane. The colorless filtrate was concentrated to afford a clear liquid with a white precipitate ($OPPh_3$) that was loaded onto a long silica column and flushed with pentane. The pentane was collected and carefully distilled off using a Vigreux column to afford a colorless liquid 2.58 g (69.2 % yield).

^{1}H NMR (500 MHz, 25 °C, C_6D_6): δ 4.98 (app s, 1H), 4.93 (app s, 1H), 2.04 (t, J_{HH} = 7.3 Hz, 2H), 1.35-1.41 (m, 2H), 1.32-1.26 (m, 6H), 0.89 (t, J_{HH} = 6.7 Hz, 3H).

^{2}H NMR (77 MHz, 25 °C, C_6D_6): δ 5.87 (m).

^{13}C{^{1}H} NMR (126 MHz, 25 °C, C_6D_6): δ 139.1 (t, J_{CD} = 22.9 Hz), 114.1, 33.9, 31.9, 29.1, 29.0, 22.8, 14.2.

B. Synthesis of Isotopically labeled Polymers

Once deuterated monomers have been synthesized the route to synthesizing deuterated polymers is as simple as substituting the labeled monomer in a typical polymerization. Freshly distilled deuterated monomers would be stored 24 hours over molecular sieves prior to polymerization. Occasionally pentane remains in the solution after distillation, in this case the polymerization is not hindered by remaining pentane so mass fraction of 1-octene is calculated from integration of the ^{1}H NMR spectrum. In an Ar dry box 25 μmol (18.8 mg) of precatalyst (tribenzyl-N-mesityl-2-methylquinolin-8-amine hafnium (IV) see Scheme 2.1 and 2.2 for more details) and 4.4 mmol (0.5 g) of 2D-1-octene was added to 20 mL of dry toluene and transferred to a Schlenk flask, removed from the dry box, and placed on a Schlenk line equipped with a vacuum line and ethylene feed. The argon atmosphere was removed by piercing the septum with a needle under excess ethylene pressure to purge the flask. The reaction is started by injecting activator solution, 27.5 μmol $B(C_6F_5)_3$ (15 mg) in 5 mL of toluene via needle. At this point the orange precatalyst solution turns to dark red, indicating the catalyst has been activated and stirring is started, allowing ethylene access to the solution. The polymerization reaction is quenched by addition of 1 mL of methanol causing the dark red color to change to yellow. After being quenched, the

reaction mixture is poured into 200 mL of 10% (v/v) HCl/MeOH and stirred overnight to remove quenched catalyst from the polymer. Isolated polymer is white or pale yellow in color and filtered from solution under vacuum and dried at 120 ℃ for two hours.

The conversion of labeled monomer to polymer was low, only 170 mg of polymer was produced (typical of reactions on this scale) and with 6.7 % (mol) of 1-octene that corresponds to only 30 mg that was polymerized (Figure 4.3).

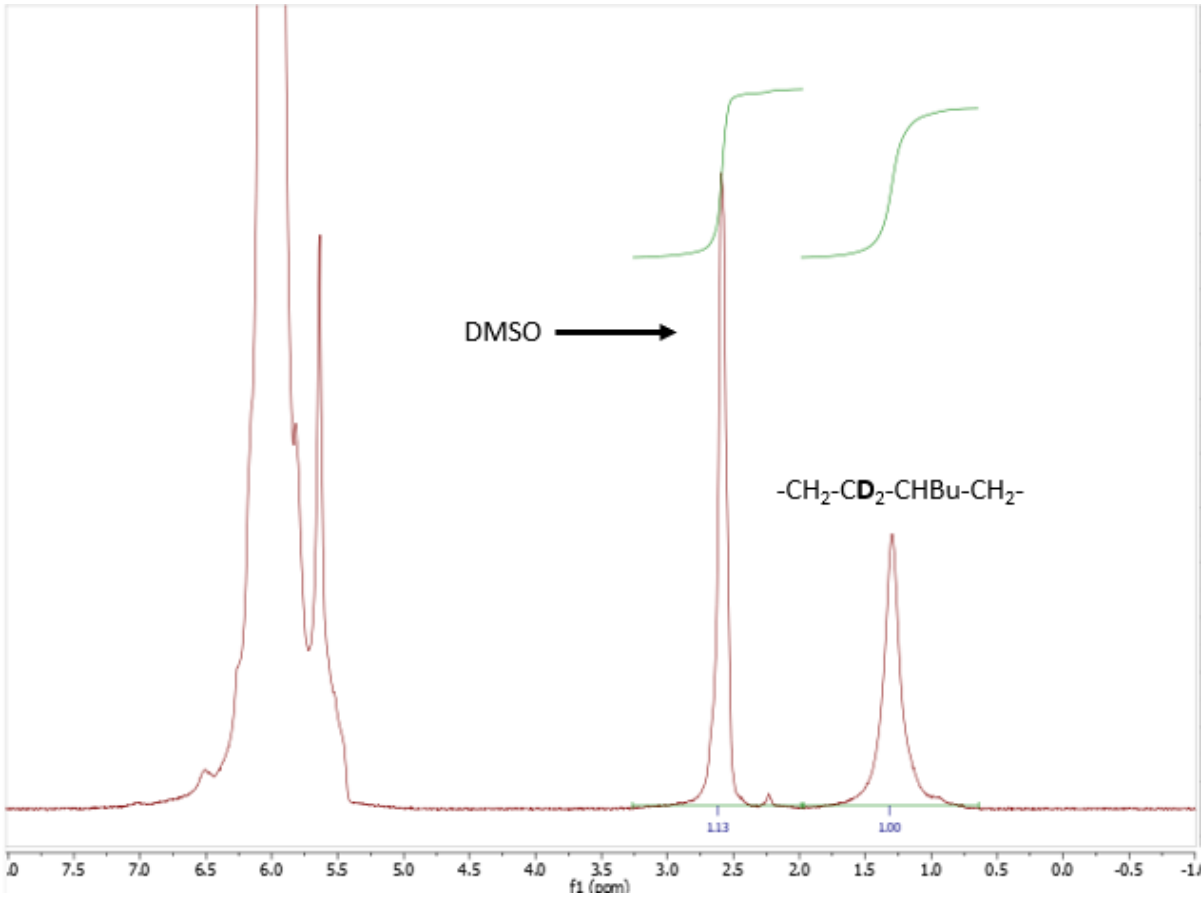

Figure 4.3 ^{2}H NMR in CD_2Cl_4 of ethylene/1,1-^{2}H-octene copolymer with DMSO added as an internal standard. Monomer incorporation can be calculated from deuterium incorporation (6.6 mol%) and was found to be in good agreement with monomer incorporation calculated from ^{13}C NMR triad analysis (6.7 mol%).

Usually, a comonomer conversion of 6% is not a problem as unlabeled α olefins are cheap and easy to obtain from chemical vendors, however, we were motivated to find other catalyst systems that could produce polymers at higher scale and higher monomer conversion for our labeled monomers. Finding a better system that incorporates more of the comonomer is currently an ongoing area of study in our lab, from literature[35] it seems that the classical Zeigler-Natta catalyst, Cp_2ZrCl_2, activated by methyl aluminum oxide (MAO) is a promising route.

D. Conclusion

The results presented here are a substantial step forward in the synthesis of deuterated alkenes via the Wittig reaction. Previous publications[34] have synthesized α olefins with high selectivity (95-98% D) in poor yields (19-40 %) and on the mg scale. Often percent yield is calculated from a crude reaction mixture via NMR rather than from the mass of an isolated product, which lowers the ability for chemists to use these labeled products in further reactions. The work presented here is the first available in the literature where synthetic methodologies for the site-specific labeling of deuterium to an α olefin was achieved on the gram scale and with isolated yields of 45-60%. This represents an important step forward for the ability of chemist to synthesize monomers, and subsequently polymers, in house from relatively cheap deuterium sources and without expensive reagents or specialized equipment. We attribute the high yields in part to the isolation of the ylide product before further reaction. When this process was attempted in one pot (as is commonly reported in literature) yields decreased by roughly half (35 %).

When interpreting NMR spectra of deuterated compounds, it is important to remember that the deuterium isotope is spin 1 in contrast to the spin ½ of the protonium isotope. This makes coupling patterns more complex to interpret because a neighboring deuterium will split peaks into three instead of two for neighboring protonium. To illustrate this elegantly Figure 4.4 shows the stacked spectra of the alkene region of 1-octene, 1,1-^{2}H-1-octene, 2-^{2}H-1-octene, and 3,3-^{2}H-1-octene from top to bottom. One can note the smearing of peaks for hydrogen adjacent to deuterium as well as the trace hydrogen residuals from incomplete deuterium incorporation.

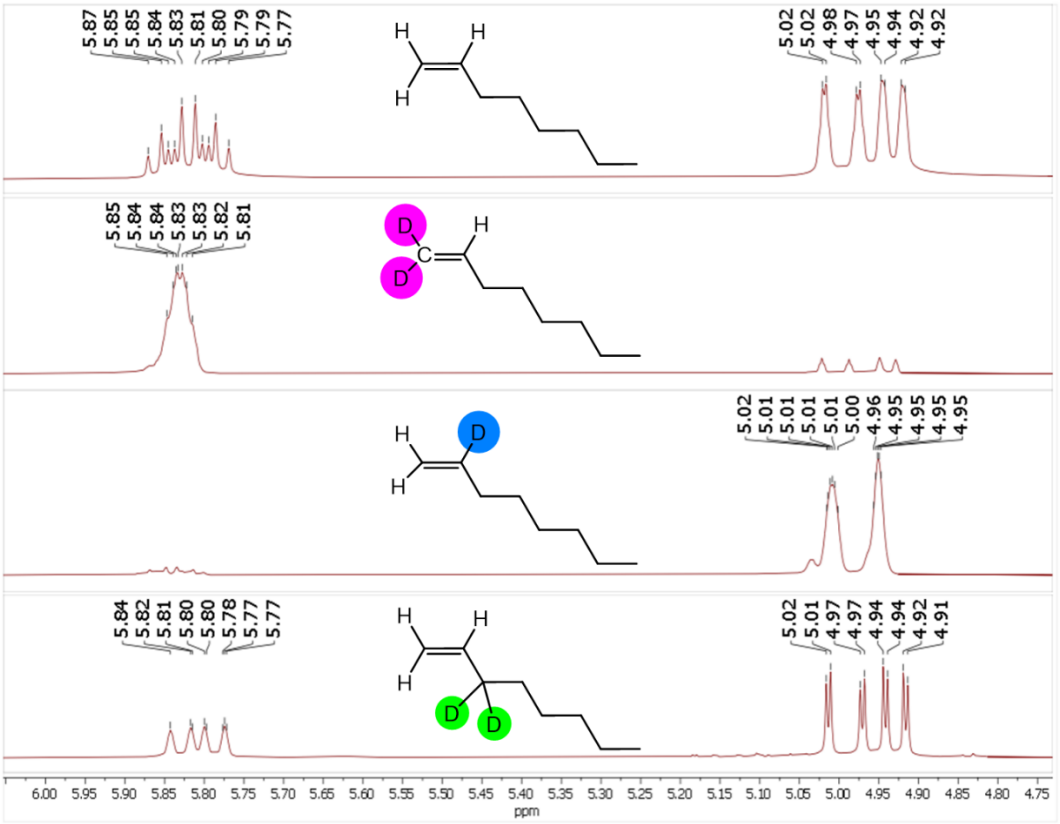

Figure 4.4 Stacked ^{1}H NMR spectra in $CDCl_3$ of the alkene region of 1-octene (top), 1,1-^{2}H-1-octene (middle top), 2-^{2}H-1-octene (middle bottom), and 3,3-^{2}H-1-octene (bottom).

Furthermore, monomer concentration of LLDPE polymers is commonly calculated from ^{13}C NMR spectra despite the low natural abundance of ^{13}C and therefore long scan times because there is significant overlap between the CH_2 and CH_3 peaks in a ^{1}H NMR spectra. By labeling a monomer with deuterium and adding an internal standard comonomer concentrations can instead be calculated from ^{2}H NMR spectra with better S/N ratios in lower times because there is no CH_2 peak overlap. This opens the opportunity to run time resolved experiments in-situ, whereas with ^{13}C NMR because of long scan times reactions are often quenched at various times and then compared. With shorter run times of ^{2}H NMR a single experiment could provide multiple time points of how the -CRD- peak evolves over the course of a reaction, representing a significant step forward for chemists attempting to understand the mechanism of LLDPE degradation.

References:

1. Annual production of plastics worldwide from 1950 to 2021, Statista, https://www.statista.com/statistics/282732/global-production-of-plastics-since-1950/ (Accessed 9-26-23)

2. Hines, R., A.; Bryant, W., M., D.; Larchar, A., W.; Pease, D., C. Synthesis of Linear Polyethylene by a Free Radical Route at Very High Pressures *Industrial and Engineering Chemisty*, 1957, Vol 49 (7), 1071-1074

3. Kim, M.; Phillips, P., J. Nonisothermal melting and crystallization studies of homogeneous ethylene/α-olefin random copolymers *J. APPL. POLYM. SCI.* 1998, Vol 70, 1893-1905

4. Cowan, A. R.; Costanzo, C. M.; Benham, R.; Loveridge, E. J.; Moody, S. C. Fungal bioremediation of polyethylene: Challenges and perspectives *Journal of Applied Microbiology,* 2021, Vol 132, 78-89

5. Singh, D.; Merrill, R. P. Molecular Weight Distribution of Polyethylene Produced by Ziegler-Natta Catalysts *Macromolecules,* 1971, Vol 4, 599-604

6. Padmanabhan, S.; Sarma, K. R.; Sharma, S. Synthesis of Ultrahigh Molecular Weight Polyethylene Using Traditional Heterogeneous Ziegler−Natta Catalyst Systems *Industrial & Engineering Chemistry Research*, 2009, Vol 48, 4866-4871

7. Rubin, I. D. Homopolymerization of ethylene and copolymerization with 1-butene in the presence of bis(cyclopentadienyl)titanium dichloride and diisobutylaluminum chloride *Journal of Polymer Science Part A-1: Polymer Chemistry*, 1967, Vol 5 (5), 1119-1128

8. Crabtree, R.H. The Organometallic Chemistry of Alkanes *Chem. Rev.* 1905, Vol 85, 245-269

9. Klosin, J.; Fontaine, P. P.; Figueroa, R. Development of Group IV Molecular Catalysts for High TemperatureEthylene-α-Olefin Copolymerization Reactions *Accounts of Chemical Research*, 2015, Vol 48, 1777-2168

10. Manz, T. A.; Caruthers, J., M.; Sharma, S.; Phomphrai, K.; Thomson, K., T.; Delgass, N., W.; Abu-Omar, M., M. Structure−Activity Correlation for Relative Chain Initiation to Propagation Rates in Single-Site Olefin Polymerization Catalysis *Organometallics,* 2012, 31, 602−618

11. Steelman, D., K.; Xiong, S.; Pletcher, P., D.; Smith, E.; Switzer, J., M.; Medvedev, G., A.; Delgass, W., N.; Caruthers, J., M.; Abu-Omar, M., M. Effects of Pendant Ligand Binding Affinity on Chain Transfer for 1-Hexene Polymerization Catalyzed by Single-Site Zirconium Amine Bis-Phenolate Complexes *J. Am. Chem. Soc.* 2013, 135, 6280−6288

12. Yang, H.; Zhang, L.; Fu, Z.; Fan, Z. Comonomer Effects in Copolymerization of Ethylene and 1-Hexene with $MgCl_2$-Supported Ziegler-Natta Catalysts: New

Evidences from Active Center Concentration and Molecular Weight Distribution *J. APPL. POLYM. SCI.* 2015

13. Smit, M.; Zheng, X.; Brull, R.; Loos, J.; Chadwick, J.; Koning, C. Effect of 1-Hexene Comonomer on Polyethylene Particle Growth and Copolymer Chemical Composition Distribution *Journal of Polymer Science: Part A: Polymer Chemistry*, 2006, Vol. 44, 2883–2890

14. Grieken, R.; Carrero, A.; Suarez, I.; Paredes, B. Effect of 1-Hexene Comonomer on Polyethylene Particle Growth and Kinetic Profiles *Macromol. Symp.* 2007, 259, 243–252

15. Cueny, E. S.; Landis, C. R. The Hafnium-Pyridyl Amido Catalyzed Copolymerization of Ethene and 1-Octene: How Small Amounts of Ethene Impact Catalysis. *ACS Catal.* 2019, 9, 3338− 3348.

16. Y. V. Kissin, R. I. Mink, T. E. Nowlin Ethylene Polymerization Reactions with Ziegler–Natta Catalysts. I. Ethylene Polymerization Kinetics and Kinetic Mechanism *Journal of Polymer Science: Part A: Polymer Chemistry*, 1999, Vol. 37, 4255–4272

17. Wu, Q.; Garcia-Penas, A.; Barranco-Garcia, R.; Cerrada, M. L.; Benavente, R.; Perez, E.; Gomez-Elvira, J. M. A New Insight into the Comonomer Effect through NMR Analysis in Metallocene Catalysed Propene–co–1-Nonene Copolymers *Polymers* 2019, 11, 1266

18. Qiao, J.; Guo, M.; Wang, L.; Liu, D.; Zhang, X.; Yu, L.; Song, W.; Liu, Y. Recent Advances in Polyolefin Technology *Polym. Chem.* 2011, 2, 1611−1623.

19. Seger, M.; Maciel, G. Quantitative 13C NMR Analysis of Sequence Distributions in Poly(ethylene-co-1-hexene) *Analytical Chemistry*, Vol. 76, No. 19, 2004

20. Switzer, J. M.; Travia, N. E.; Steelman, D. K.; Medvedev, G. A.; Thomson, K. T.; Delgass, W. N.; Abu-Omar, M. M.; Caruthers, J. M., Kinetic Modeling of 1-Hexene Polymerization Catalyzed by Zr(tBu-ONNMe$_2$O)Bn$_2$/B(C$_6$F$_5$)$_3$. *Macromolecules* Vol. 45, No. 12, 4978-4988, 2004

21. Pletcher, P. D.; Switzer, J. M.; Steelman, D. K.; Medvedev, G. A.; Delgass, W. N.; Caruthers, J. M.; Abu-Omar, M. M., Quantitative Comparative Kinetics of 1-Hexene Polymerization across Group IV Bis-Phenolate Catalysts. *Acs Catalysis*, Vol. 6, No. 8 5138- 5145. 2016

22. Steelman, D. K.; Pletcher, P. D.; Switzer, J. M.; Xiong, S.; Medvedev, G. A.; Delgass, W. N.; Caruthers, J. M.; Abu-Omar, M. M. Comparison of Selected Zirconium and Hafnium Amine Bis- (Phenolate) Catalysts for 1-Hexene Polymerization. *Organometallics* 2013, 32, 4862−4867.

23. Caldera, A.; Soares, J. B. P.; DesLauriers, P. J.; Fodor, J. S. Ethylene/1-Hexene Polymerization with Bis(Cyclopentadienyl) Hafnium(IV) Dichloride: A Fundamental Polymerization Kinetics Model. *J. Catal.* 2019, 375, 140−154.

24. Case, L., C.; Atlas, J., D. Hydrogen and Deuterium Exchange of Polypropylene *Journal of Polymer Science* 1960, 45, 146, 289-563

25. Shin, K.; Bukhov, S.; Taichen, J.; Huh, J.; Hwang, Y.; Mok, S.; Dobriyal, P.; Thiyagarajan, P.; Russell, T. Enhanced mobility of confined polymers *Nature Materials* 2007, Vol 6, 961-965

26. König, N.; Willner, L.; Pipich, V.; Mahmoudi, N.; Lund, R. Tale of Two Tails: Molecular Exchange Kinetics of Telechelic Polymer Micelles *Physical Review Letters* 2020, Vol 124 (19), 197801-197807

27. Plastic Waste Worldwide, Statistics and Facts, Statista, https://www.statista.com/topics/5401/global-plastic-waste/#topicOverview (Accessed 10-17-23)

28. Weddin, M., A.; Murata, K., K.; Sakata, Y. Thermal and Catalytic Degradation of Structurally Different types of Polyethylene into Fuel Oil *Polymer Degradation and Stability*, 1997, 54, 37-44

29. Park, D., W.; Hwang, E., Y.; Kima, J., R.; Choi J., K.; Kima Y., A.; Woo, H., C. Catalytic degradation of polyethylene over solid acid catalysts *Polymer Degradation and Stability*, 1999, 65, 193-198

30. Tennakoon, A.; Wu, X.; Paterson, A., L.; Patnaik, S.; Pei, Y.; LaPointe, A., M.; Ammal, S., C.; Hackler, R., A.; Heyden, A.; Slowing, I., I.; Coates, G., W.; Delferro, M.; Peters, B.; Huang, W.; Sadow A., D.; Perras, F., A. Catalytic upcycling of high-density polyethylene via a processive mechanism *Nature Catalysis*, 2020, 3, 893–901

31. Guironnet, D.; Peters, B. Tandem Catalysts for Polyethylene Upcycling: A Simple Kinetic Model *Journal of Physical Chemistry* 2020, 124, 3935-3942

32. Kolganov, A., A.; Sreenithya, A.; Pidko, E., A. Homogeneous Catalysis in Plastic Waste Upcycling: A DFT Study on the Role of Imperfections in Polymer Chains *ACS Catal.* 2023, 13, 13310–13318

33. Uenoa, T.; Nakashimab, E.; Takeda, K. Quantitative analysis of random scission and chain-end scission in the thermal degradation of polyethylene *Polymer Degradation and Stability,* 2010, Vol 95, 1862-1869

34. Atinson, J, G.; Fisher, M., H.; Iorlei, D.;Xioizse, A., D.; Stuart, R., S. Synthesis of isotopically labelled olefins via the Wittig reaction *Canadian Journal of Chemistry*, 1965, Vol 33, 1614-1624

35. Lee, H., W.; Ahn, S., H.; Park, Y., H. Copolymerization characteristics of homogeneous and in-situ supported $[(CH_2)_5(C_5H_4)_2][(C_9H_7)ZrCl_2]_2$ catalyst *Journal of Molecular Catalysis A: Chemical*, 2003, Vol 194, 19–28